Session II

Nuclear data validation and benchmarks

Chair: Krzysztof Drozdowicz

Final results of the "Benchmark on computer simulation of radioactive nuclides production rate and heat generation rate in a spallation target"

J. Janczyszyn, W. Pohorecki, G. Domańska
AGH – University of Science and Technology, Al. Mickiewicza 30, 30-059 Krakow, Poland,

Benchmark participants:
R.J. Maiorino[1], J.-Ch. David[2], F.A. Velarde[3], G. Domańska, W. Pohorecki
[1]IPEN, Brazil,
[2]CEA, France,
[3]CIEMAT, Spain

Abstract

Selection of the model or code most useful for the ADS target activation calculations and, if such a tool is not yet available, the indication of the main deficiencies of the existing tools was undertaken. Also the proper calculation of the spallation target heating, both during its exposition to the beam and after its switch off was analysed. Results of the measurement of radioactivity induced in massive Pb target were applied as reference to the presented benchmark calculations. For the heat generation in the target only the intercomparison of calculations was assumed. The specific goals of the benchmark were: calculation of the long lived residuals production rate and activity in a lead target after its irradiation with 660 MeV protons, comparison of the results with the measured ones for the isotopes: ^{46}Sc, ^{59}Fe, ^{60}Co, ^{65}Zn, ^{75}Se, ^{83}Rb, ^{85}Sr, ^{88}Y, ^{88}Zr, ^{95}Nb, ^{95}Zr, ^{102m}Rh, ^{102}Rh, ^{110m}Ag, ^{121m}Te, ^{121}Te, ^{139}Ce, ^{172}Hf, ^{172}Lu, ^{173}Lu, ^{175}Hf, ^{183}Re, ^{185}Os, ^{194}Au, $^{194m2}Ir$, ^{195}Au, ^{203}Hg, ^{207}Bi, *calculation of the heating rate in the target and comparison of the results of calculations.*

Introduction

Deployment of Accelerator Driven System (ADS) is regarded as an interesting option of improving safety of nuclear power by the spent fuel transmutation. Actinide recycling can reduce the need for the large-scale repository of waste. One of the essential parts of ADS is the spallation target serving as the external neutron source of the subcritical core. The study of ADS operation and maintenance includes also the analysis of the build-up and decay of the target radioactivity and heating. The heating resulting from the beam particles and decay of radioactive nuclides. Both, the radioactivity and heating, can be calculated with the use of standard computational tools such as MCNPX [1], FLUKA [2,3] and others. However, not always the calculation methodology is straightforward and unambiguous. In calculation of radioactivity for the intermediate and high-energy range of particles (~ 20 - 1500 MeV) a number of physical models of nuclear interactions between the incident particle and nucleus are at hand (MCNPX). The selection of the model or code most useful for the ADS calculations and, if such a tool is not yet available, the indication of the main deficiencies of the existing tools, is undertaken as a task in the NUDATRA domain of the Integrated Project EUROTRANS. It is also a part of the IAEA Coordinated Research Project on Analytical and Experimental Benchmark Analyses of Accelerator Driven Systems. The proper calculation of the spallation target heating, both during its exposition to the beam and after its switch off is of importance for the designing of the XT-ADS and EFIT systems [4]. The experiment devoted to the measurement of axial distributions of radionuclide activity induced in massive Pb target was conducted at the Dzhelepov Laboratory of Nuclear Problems in JINR Dubna (Russia) [5-7] and its results were applied as reference to the presented benchmark calculations. There was no experiment conducted within this research, resulting in the respective measurement of heat generation or temperature distribution in the target. Therefore only the intercomparison of results of calculations was assumed. Thus the specific goals of the benchmark were: calculation of: the long lived residuals production rate during the lead target irradiation and their activity at 219 days after the irradiation end, in 32 pieces of Pb samples, distributed inside the target, and in the whole target; comparison of these results with the measured ones for the following isotopes: ^{46}Sc, ^{59}Fe, ^{60}Co, ^{65}Zn, ^{75}Se, ^{83}Rb, ^{85}Sr, ^{88}Y, ^{88}Zr, ^{95}Nb, ^{95}Zr, ^{102m}Rh, ^{102}Rh, ^{110m}Ag, ^{121m}Te, ^{121}Te, ^{139}Ce, ^{172}Hf, ^{172}Lu, ^{173}Lu, ^{175}Hf, ^{183}Re, ^{185}Os, ^{194}Au, ^{194m2}Ir, ^{195}Au, ^{203}Hg, ^{207}Bi; calculation of the heating rate and its distribution in the target both, during exposition to the proton beam and after its switch-off, comparison between the results of calculations of heating rate. The benchmark was presented in Nice during the International Conference on Nuclear Data for Science and Technology 2007 [8]. Also partial results were presented on the Physor 2008 conference [9].

Analysis of the benchmark results for activation

Results for the whole target

Instantaneous isotope production rate

First part of the benchmark analysis was devoted to testing the calculation results for consistency. Results of instantaneous production rate for 24 nuclides, obtained with the use of each physical model (Bertini, CEM, INCL4 and Isabel) were compared (Figure 1). Generally the received results are consistent (Table 1). In cases when the consistency is worse one can observe either the spread of results higher than the respective uncertainties or systematic difference for selected nuclides. Instantaneous production rate results in the whole target are consistent for majority of participants and for all models. Differences between models are significant.

Figure 1: Examples of the comparison of results of the instantaneous production rate of the radioactivity induced in the whole target

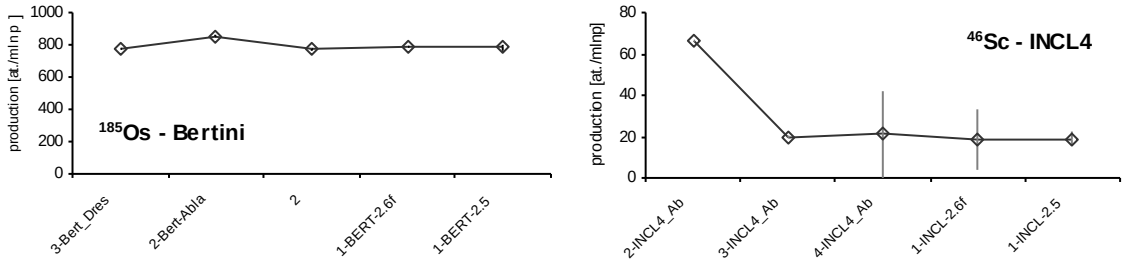

Table 1: Results of the comparison of instantaneous nuclide production rate

	Model:	Bertini	CEM	INCL4	Isabel
	Total number of results	Number of nuclides showing consistent results			
All nuclides	24	17	22	20	18
Light (A ≤ 60)	3	2	2	3	3
Fission products (60 < A < 140)	11	10	11	10	9
Heavy spallation residues (A ≥ 140)	9	5	9	7	6
^{207}Bi	1	-	-	-	-

Activity with account of the decay during and after activation

To compare the experimental results with the calculated ones one should recalculate the instantaneous production rates of the respective nuclide and its all predecessors for the moment of measurement. It should account both for the growth and decay during activation and the decay after activation end.

Examples of the comparison of results for the whole target are presented in Figure 2 while all ratios C/E (calculation to experiment) in Table 2

Figure 2: Examples of comparison of calculation results of the whole target activity for selected nuclides with account of the decay during and after activation

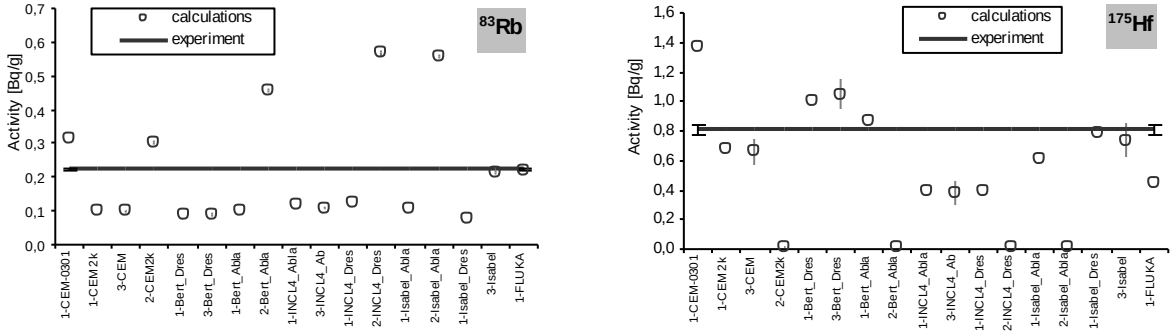

For the statistical analysis of the results the D and H coefficients were applied (Eq. (1))

$$D = \frac{\sum_{i=1}^{n} \left| 1 - \frac{C}{E} \right|}{n}, \qquad H = \sqrt{\frac{1}{n} \sum_{i=1}^{n} \left(\frac{E_i - C_i}{S_{E,i} + S_{C,i}} \right)^2} \tag{1}$$

where *n* – number of compared results due to different isotopes or participants and models. In calculations of the coefficient for isotopes the outlying results were omitted while when comparing models and participants the results of participant 2 were not evaluated. Also the results for isomeric states and respective nuclides were not considered due to the lack of separated production rates for the ground and excited state formation in majority of supplied data. Results are presented in Table 2.

Table 2: Cumulative results of the C/E ratio for the radionuclides activity of the whole target with account of the decay during and after activation

Participant No and model/code	C/E															
	Nuclide															
	^{60}Co	^{65}Zn	^{83}Rb	^{85}Sr	^{88}Y	^{95}Nb	^{102}Rh	$^{102m+g}$Rh	$^{121m+g}$Te	^{173}Lu	^{175}Hf	^{183}Re	^{185}Os	^{194}Au/Hg	^{203}Hg	^{207}Bi
1-CEM-0301	0.65	1.67	1.40	1.19	1.31	0.57	-	-	-	1.58	1.70	1.68	1.06	0.82	0.55	1.42
1-CEM2k	0.40	1.43	0.45	0.45	0.47	0.23	0.40	0.21	0.37	0.72	0.84	1.34	1.10	1.12	0.49	1.66
3-CEM	0.41	1.45	0.44	0.46	0.50	0.24	0.40	0.20	-	0.76	0.82	1.34	1.11	1.64	0.77	1.77
2-CEM2k	9.81	1.42	1.35	69.24	0.96	8.63	0.25	0.13	60.80	0.01	0.02	0.19	0.04	8307.88	0.64	1.78
1-Bert_Dres	0.41	1.20	0.39	0.33	0.38	0.23	0.42	0.22	0.51	1.30	1.24	1.53	1.05	0.85	1.30	1.40
3-Bert_Dres	0.46	1.41	0.39	0.32	0.38	0.24	0.42	0.22	-	1.36	1.29	1.54	1.07	1.35	1.44	1.47
1-Bert_Abla	0.43	0.61	0.44	0.37	0.38	0.36	0.67	0.34	0.42	0.99	1.07	1.46	1.16	0.94	1.32	1.06
2-Bert_Abla	7.94	0.84	2.05	68.82	1.17	8.33	0.41	0.21	65.80	0.01	0.02	0.24	0.06	8021.72	1.20	1.09
1-INCL4_Abla	0.51	0.54	0.53	0.45	0.44	0.64	0.84	0.43	0.59	0.38	0.49	0.96	0.82	0.93	1.61	1.17
3-INCL4_Abla	0.55	0.62	0.49	0.48	0.48	0.67	0.94	0.48	-	0.42	0.47	0.96	0.83	1.38	1.70	1.22
1-INCL4_Dres	0.51	0.47	0.57	0.44	0.45	-	0.89	0.46	0.56	0.38	0.48	0.97	0.82	0.92	1.62	1.17
2-INCL4_Dres	11.35	0.99	2.53	69.60	1.55	8.33	0.53	0.27	56.84	0.01	0.01	0.17	0.04	9185.42	1.65	1.18
1-Isabel_Abla	0.39	0.58	0.48	0.42	0.45	0.51	0.85	0.44	0.51	0.65	0.75	1.29	1.08	1.00	1.02	1.85
2-Isabel_Abla	11.47	0.96	2.48	66.71	1.42	8.44	0.49	0.25	57.76	0.01	0.01	0.22	0.06	6715.72	1.22	1.98
1-Isabel_Dres	0.42	1.16	0.33	0.28	0.35	0.23	0.41	0.21	0.47	0.93	0.97	1.44	1.04	0.92	1.30	1.40
3-Isabel	1.00	1.25	0.96	0.79	0.84	0.80	1.38	0.71	-	0.94	0.91	1.26	1.02	1.55	0.83	1.15
1-FLUKA	0.72	1.00	0.98	0.85	0.96	0.55	-	-	-	0.48	0.56	0.90	0.75	1.02	0.62	1.01

10%>C/E>0%

20%>C/E>10%

0.2 > C/E > 5

Examination of the Table 2 and qualitative comparison of calculated activities with the experimental ones show for the whole target, for different models:

- the worst performance of Bertini-Dresner (~ 12% acceptable results, below 20% difference)
- better of CEM, INCL4, ISABEL-Dresner and Bertini-Abla (~20-30%)
- the best but still unsatisfactory of ISABEL-Abla and FLUKA (~45 %)

Analysis of the quality of 13 calculated results for different nuclides (excluding these strongly outlying from unity - marked in the Table 2) show:

- the best performance for ^{185}Os and ^{194}Au/^{194}Hg, (12 and 9 results within 20%, respectively)
- for ^{183}Re, ^{175}Hf and ^{207}Bi only 4 – 6 results within this limit
- for nuclides from ^{60}Co to ^{121}Te almost all calculations underestimated
- for heavier mainly overestimated.

The quantitative analysis with the use of coefficient D, reflecting the absolute deviation of the C/E ratio from unity (Table 3), confirms the best performance of Isabel model and FLUKA code and worst of Bertini-Dresner and CEM 2k models. Among isotopes the D values for ^{185}Os and ^{194}Au/^{194}Hg are the lowest

Table 3: Values of the D coefficient for models and nuclides

Participant code - model	D	Nuclide	D
1-CEM-0301	0.42	^{60}Co	0.47
1-CEM 2k	0.48	^{65}Zn	0.32
3-CEM	0.49	^{83}Rb	0.61
1-Bert_Dres	0.46	^{85}Sr	0.50
3-Bert_Dres	0.50	^{88}Y	0.44
1-Bert_Abla	0.38	^{95}Nb	0.56
1-INCL4_Abla	0.39	^{173}Lu	0.35
3-INCL4_Ab	0.39	^{175}Hf	0.31
1-INCL4_Dres	0.39	^{183}Re	0.38
1-Isabel_Abla	0.39	^{185}Os	0.11
1-Isabel_Dres	0.43	^{194}Au/Hg	0.21
3-Isabel	0.19	^{203}Hg	0.38

Results for the distribution along the target

Example of the comparison of results for the distribution along the target is presented in Figure 3 while the ratios C/E (calculation to experiment) in Figure 4.

The quantitative evaluation, of results for all 22 analysed nuclides and 4 physical models of the spallation reaction, was done with the use of the D and H coefficients (Eq. (1)). The coefficient H represents the weighed quadratic average of absolute distance of points from the line representing the equality of measured and calculated results (as can be seen on the right side graph in Figure 4). As the weight the reciprocal of the sum of standard deviations of experimental and calculated result was applied. The calculated values of coefficients D and H are presented in Table 4.

Analysis of the values of coefficient D allows for the following observations:

- average values for all nuclides differ only slightly;
- the Isabel model seems to be better (D = 0.40) and the Bertini-Dresner worse (D = 0.56) then the two others,
- only ~12 % of calculated results from all models differ from experimental ones by less than 20 %.

Figure 3: Cumulative comparison of calculated (weighed mean) and measured specific activity distribution along the target with the account of decay during and after activation for different physical models applied in calculations

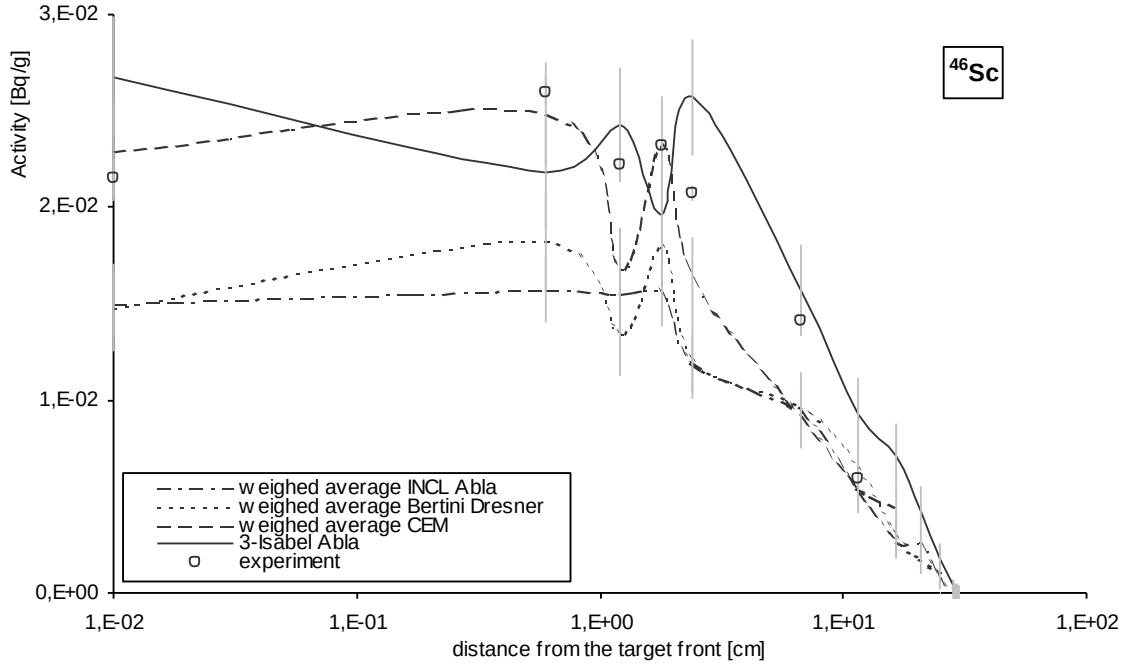

Figure 4: Comparison of the experimental and calculated distributions of 95Nb (specific activity in Bq/g) along the target. The calculated values are weighed averages of results from participants.

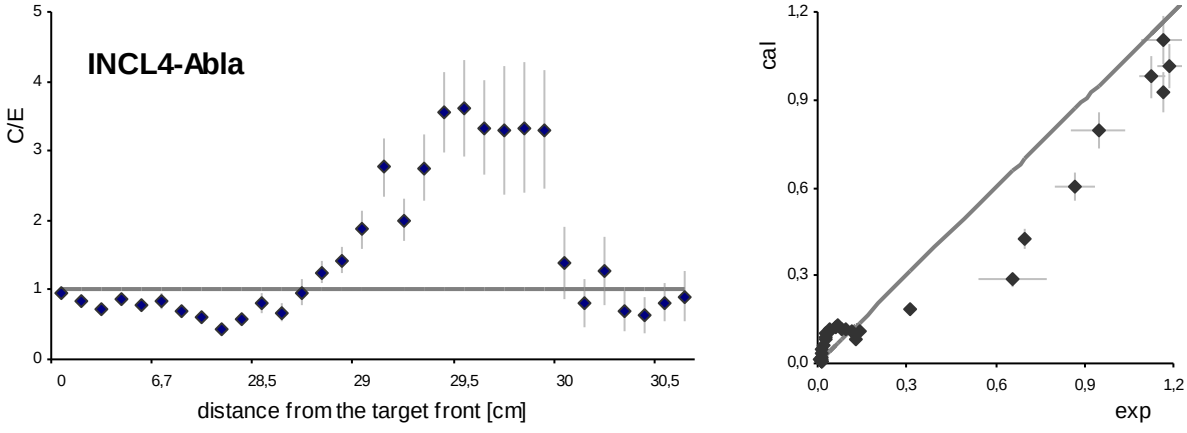

Table 4: Values of the D and H coefficients for models and nuclides*

Nuclide	CEM	BerDre	INCL4Abla	Isabel		CEM	BerDre	INCL4Abla	Isabel
	D					H			
Sc46	0.117	0.294	0.316	0.229		0.76	1.76	2.20	0.99
Fe59	0.257	0.276	0.179	0.304		2.55	2.02	1.97	2.02
Co60	0.587	0.588	0.530	0.223		4.64	4.71	4.72	1.73
Zn65	0.816	0.850	0.926	0.848		2.60	2.36	3.48	2.44
Se75	0.215	0.566	0.284	0.593		1.16	3.25	2.51	2.57
Rb83	0.565	0.584	0.443	0.148		4.99	5.71	4.41	1.14
Sr85	0.781	0.559	0.492	0.246		4.13	4.96	4.08	1.76
Y88	0.593	0.697	0.503	0.408		5.14	5.09	5.29	2.99
Zr88	0.137	0.313	0.576	0.210		0.97	2.55	5.24	1.65
Nb95	0.862	0.805	0.748	0.750		9.66	6.19	2.44	2.09
Zr95	0.846	0.755	0.900	0.852		9.78	6.77	4.44	3.58
Ce139	0.474	0.095	0.075	0.112		2.07	0.44	0.42	0.38
Hf172	0.627	0.906	0.404	0.480		4.26	5.85	3.24	2.76
Lu172	0.331	0.596	0.474	0.263		1.50	2.85	2.52	0.61
Lu173	0.350	0.473	0.559	0.204		3.30	1.92	3.07	1.03
Hf175	0.273	0.380	0.511	0.271		1.08	1.02	2.45	0.58
Re183	0.347	0.469	0.174	0.349		1.81	2.01	1.15	1.00
Os185	0.231	0.244	0.363	0.270		0.74	0.65	1.50	0.86
Au194	0.502	0.287	0.198	0.618		3.74	1.52	0.97	3.69
Au195	0.281	0.144	0.606	0.587		1.70	1.27	5.25	2.37
Hg203	0.424	1.487	0.571	0.178		4.03	6.45	5.05	1.25
Bi207	1.134	0.946	0.420	0.612		15.19	13.93	6.13	9.53
average	0.49	0.56	0.47	0.40		3.90	3.79	3.30	2.14

*Each value represents all points of one distribution along the target.

0.10 > D > 0 **0.2 > D ≥ 0.1** **1.0 > H > 0** **2.0 > H ≥ 1.0**

When the difference is related to the result standard deviation, both from calculation and experiment (in coefficient H) the differentiation between models and nuclides looks more distinct:

- the Isabel model yields best results – the average difference is slightly larger than 2 standard deviation while for the other 3 models it is between 3.3 (INCL4-Abla) and 3.9 (CEM),
- for Isabel model over 55 % of values is smaller than 2 and for the other models only ~33 %.

The distributions along the target contain also some information about the proton energy influence on the results of calculation. Samples placed in different distance from the target front were irradiated with protons (mainly) of different spectra. Based on the approximate dependence of the respective distribution peak energy on the sample position one can observe the following general regularities:

- best (but not always satisfactory) results of calculations for proton energy above ~120 MeV (on the average for all measured nuclides) are obtained for the Isabel model, while below this energy results from INCL4-Abla are the best but only slightly better than that from Bertini-Dresner,
- calculated results are in satisfactory agreement with the experimental ones only for proton energy above ~ 460 MeV.

This is more difficult to recognize clear regularities when looking on the results from the point of view of the measured radionuclide or group of them, for the whole proton energy range on average. What can be observed is:

- the quality of results calculated with the use of Isabel model prevails over the one from other models for: ^{83}Rb, ^{85}Sr, ^{139}Ce, ^{172}Hf, ^{172}Lu, ^{173}Lu, ^{175}Hf, ^{183}Re, ^{195}Au, ^{203}Hg and ^{207}Bi,
- no model is satisfactory, even approximately, for such nuclides as: ^{60}Co, ^{65}Zn, ^{88}Y, ^{88}Zr, ^{95}Nb, ^{95}Zr, ^{172}Hf, and ^{203}Hg,
- other models (but Isabel) produce relatively good results for certain nuclides, i.e.: INCL4-Abla for ^{59}Fe, ^{139}Ce and ^{183}Re, CEM for ^{185}Os, Bertini-Dresner for ^{194}Au.

Analysis of the benchmark results for heating

The only goal to be achieved from this part of the benchmark is the comparison of calculation results and analysis of their compatibility among themselves and with earlier expectations. For this a similar target was designed with slightly different structure of cells [9].

Power released in the target during the beam operation

The calculation results for the whole target heating rate are presented in the Table 5. The assumed beam parameters were 1 mA continuous Gaussian beam of 660 MeV protons. The results from all participants are consistent. Around 400 kW (ca 60 % of the beam power) is released. Only small differences (ca 2 % spread) are observed between results from different models.

Table 5: Comparison of calculated results of the whole target heating power [kW] by a 1 mA beam of 660 MeV protons

Participant No	Physical model						Remark
	Bertini Abla	Bertini Dresner	INCL4 Abla	CEM	Isabel Abla	Isabel Dresner	
1	387.6	392.1	391.7	391.7	391.9	395.8	MCNPX 2.2.3
3	-	389.9	399.3	369.5	397.2	-	MCNPX 2.5.0
5	-	-	405.0	396.0	-	-	MCNPX 2.5.0

Figure 5. Distributions of the total heating power in the target calculated with the use of INCL4-Abla model. The numbers on axis x represent target cells of different thickness in the longitudinal direction.

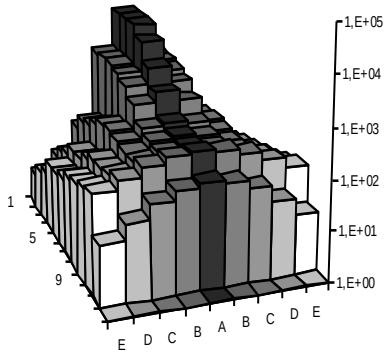

Figure 6. The distribution of relative total heating power spread between results obtained with models CEM, Bertini-Dresner, INCL4-Abla and Isabel. The numbers and letters on axes x and y represent target cells.

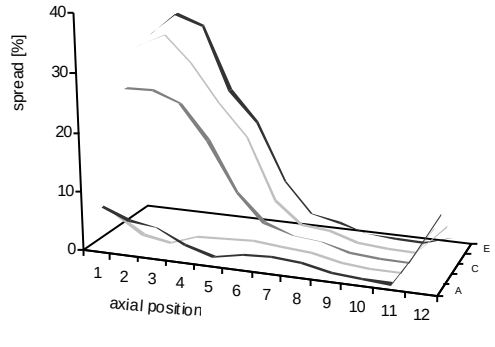

Example of the longitudinal and radial heating distribution is presented in Figure 5. Comparison of the distributions yielded by different spallation reaction models show serious differences. One example is presented in Figure 6. For the major part of the target the spread between the most differing models is smaller than 10 %. However there are regions where spread higher than 40 % is obtained. These are the most radially outside parts of the target front and at the target end behind the primary proton range. One can suspect in both cases the different "behaviour" of secondary particles in different simulation models. Difference in evaluation of such parameters of secondary particles as their energy and direction as well as their production cross-sections can cause the difference.

Conclusions

Results from the limited number of laboratories that took part in the exercise still present a clear picture of the situation regarding the thick target activation simulation. However, the relatively small amount of the used experimental data may restrict the general validity of the below conclusions.

The physical models applied for the *calculation of thick lead target activation do not produce satisfactory results* for the majority of analysed nuclides, however one can observe better or worse quantitative compliance with the experimental results. Analysis of the quality of calculated results show the best performance for heavy nuclides ($A \cong 170 - 190$). For intermediate nuclides ($A \cong 60 - 130$) almost all are underestimated while for $A \cong 130 - 170$ mainly overestimated.

The *shape of the activity distribution* in the target *is well reproduced* in calculations by all models but the numerical comparison shows similar performance as for the whole target. The Isabel model yields best results. Analysing the distributions of C/E ratio along the target length as a function of the dominating proton energy one can observe the best (but not always satisfactory) results for proton energy above ~120 MeV for the Isabel model. Below this energy results from INCL4-Abla are the best but only slightly better than that from Bertini-Dresner. Calculated results are in satisfactory agreement with the experimental ones only for proton energy above ~ 460 MeV.

The situation is different for calculations of heating. For the *whole target heating rate the results* from all participants *are consistent*. Only small differences are observed between results from physical models.

For the *heating distribution in the target* it looks not quite similar. The quantitative comparison of the distributions yielded by different spallation reaction models shows for the major part of the target no serious differences – generally below 10%. However, in the most outside parts of the target front layers and the part of the target at its end behind the primary protons range spread higher than 40 % is obtained.

Acknowledgements

The authors appreciate the efforts and support of all the scientists and institutions involved in EUROTRANS and the presented work, as well as the financial support of the European Commission through the contract FI6W-CT-2004-516520 and Polish Ministry of Science and Higher Education (contract No 35/6. PR UE/2006/7 from 5th July 2006). Thanks are also due to the IAEA for financing the Coordinated Research Project *on Analytical and Experimental Benchmark Analyses of Accelerator Driven Systems* through *the contract* No. 13395/R0/2004.

References

[1] Waters, L., *MCNPX User's Manual and Extensions Version 2.5.0*, LA-UR-05-2675 (2005).

[2] Fasso, A., *et al.*, "The physics models of FLUKA: status and recent developments", *Computing in High Energy and Nuclear Physics Conference (CHEP2003),* La Jolla, CA, USA (2003).

[3] Fasso, A., *et al.*, *FLUKA: a multi-particle transport code*, CERN-2005-10, INFN/TC_05/11, SLAC-R-773, (2005).

[4] Knebel, J., *et al.*, "European research programme for the transmutation of high level nuclear waste in an accelerator driven system (EUROTRANS)", *Proceedings of the Ninth International Exchange Meeting on Partitioning & Transmutation,* p. 25, Nimes, France (2006).

[5] Janczyszyn, J., *et al.,* "Experimental Assessment of Radionuclide Production in Materials Near to the Spallation Target", *Proceedings of the ANS Topical Meeting on Accelerator Applications/ Accelerator Driven Transmutation Technology and Applications - AccApp/ADTTA'01*, Reno, USA, CD, ISBN: 0-89448-666-7, 200284 (2001).

[6] Pohorecki, W., *et al.*, "Measurements of production and distribution of radionuclides in the spallation target", *PHYSOR 2002 Int. Conf. on the New Frontiers of Nuclear Technology: Reactor Physics, Safety and High-Performance Computing*, Seoul, CD (2002).

[7] Pohorecki, W., *et al.,* "Spatial distributions of reaction rates inside and next the spallation neutron source", *Proc. Int. Workshop on P&T AND ADS DEVELOPMENT,* SCK·CEN, Belgium, CD, ISBN 9076971072, BLG-959 (2003).

[8] Pohorecki, W., *et al.*, "Thick lead target exposed to 660 MeV protons: benchmark model on radioactive nuclides production and heat generation, and beyond", *Proc. Int. Conf. Nuclear Data for Science and Technology,* Nice, France (2007).

[9] Pohorecki, W., *et al.*, "Benchmark on computer simulation of radioactive nuclides production rate and heat generation rate in a spallation target", *Proc. Int. Conf. Physics of Reactors "Nuclear Power: A Sustainable Resource"*, Interlaken, Switzerland, CD, ISBN 978-3-9521409-5-6, paper #240 (2008)

Testing of nuclear data by comparison of measured and calculated leakage neutron and photon spectra for nickel spherical assembly

B. Jansky,[1] **Z. Turzik,**[1] **E. Novak,**[1] **M. Svadlenkova,**[1] **M. Barta,**[1] **L.A. Trykov†,**[2] **A.I. Blokhin**[2]
[1]Research Centre Rez Ltd., Czech Republic
[2]Institute for Physics and Power Engineering, Obninsk, Russia

Abstract

The leakage neutron and gamma spectra measurements have been done on benchmark spherical assembly - nickel sphere with diameter of 50 cm. The Cf-252 neutron sources with different emissions were placed into the centre of sphere. The proton recoil method was used for neutron spectra measurement using stilbene crystals and hydrogen proportional counters. The neutron energy range of spectrometer was from 0.02 to 17 MeV. The gamma pulse shape discrimination method has been applied in stilbene measurements. The gamma energy range of spectrometer was from 0.1 to 10 MeV. The fine structure of gamma spectrum was measured by HPGe spectrometer. The experimental data were compared to results of transport calculations based on different evaluated nuclear data libraries (ENDF/B-VII.0, JENDL-3.3, JENDL-4.0, CENDL-3.1, JEFF-3.1.1, TENDL-2008, TENDL-2009). The continuous energy Monte Carlo transport calculation code MCNP-4C was employed for the calculations. Main observed differences between experiments and transport calculations are discussed. Gamma fluence absolute values for discrete gamma-lines with energy 511, 1333 and 1454 keV were compared with calculations. The comparison of the calculations with measurements performed by the scintillation detector of the stilbene type is also included.

Introduction

Neutron and gamma field parameters were studied on benchmark spherical assembly - nickel sphere with diameter of 50 cm. The Cf-252 neutron sources were placed into the centre of nickel sphere. The measurement results were compared with parallel calculations using seven different data libraries in MCNP code. The following data libraries were used:

ENDF/B-VII.0, JENDL-3.3, JENDL-4.0, JEFF-3.1.1, CENDL-3.1, TENDL-2008, TENDL-2009.

The measurement results can serve as qualitative and partly also quantitative verification of various data libraries. The preliminary results concerning neutron emission spectra for nickel and also for iron spheres were presented in [1-3].

Experimental assembly

The experimental assemblies is formed by the pure nickel sphere with diameter of 50 cm with neutron source in centre, see Figure 1. Nickel sphere has the following composition:

Impurities (in sample of Ni)	**Al**	**B**	**Cd**	**Cr**	**Mn**	**Fe**	**Mo**	**Cu**	**W**	**Gd**
Concentration, [μg/g]	1020	0,05	0,08	219	185	2095	71,2	96,7	0,84	0,01

Neutron and gamma spectra were measured in two distances:

R=100 cm, abbrev. of the assembly is **NI DIA50, R100**, shadow cone used (background is subtracted),

R=28 cm, abbrev. of the assembly is **NI DIA50, R28**, without shadow cone (background is included).

Figure 1: Basic scheme of n,g-spectrum measurement. The sphere center is 200 cm above the concrete floor. In the figure is g-spectrum measurement by HPGe.

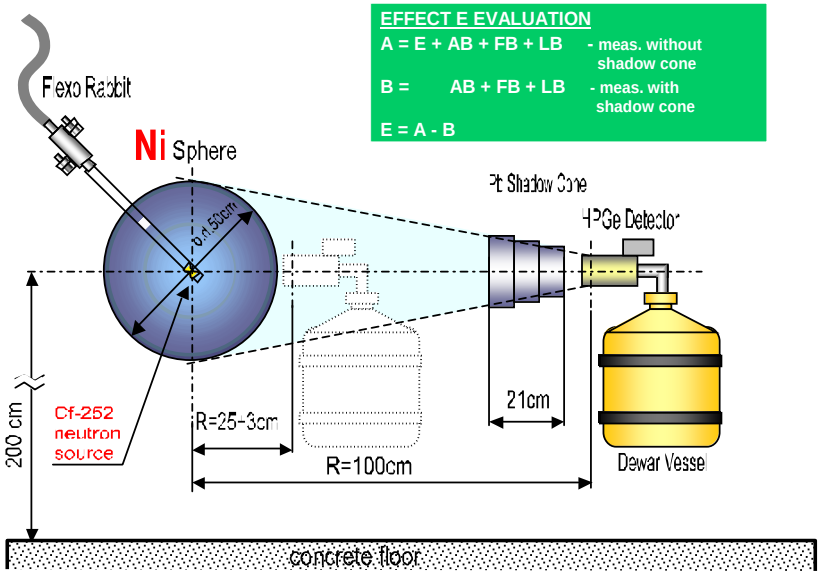

Methodology of calculation and measurement

The spherical shape of assembly and spherical neutron source is used because this geometry represents the simplest one-dimensional (1D) calculation task. As a matter of fact, the assembly is a 3D object. The methodology used for nickel sphere was identical for iron spheres measurement and calculation performed earlier [4].

The background of the measured field is determined by additional measurement performed with shielding cone (Fe + borated PE for neutrons and Pb for gamma). The shielding cone has to shield corresponding space angle to measure only all unwelcome scattered neutrons and laboratory background neutrons and gamma. It was used for R=100 cm only. The thickness of shielding cones not allow their placement in front of detectors for R=28 cm.

Neutron spectrometry

The proton recoil method was used for neutron spectra measurement as well as main methods. Hydrogen proportional counters (HPC, En=0.01-1.3 MeV) and scintillation detector of stilbene (En=0.1-17 MeV), [5], were used for neutron spectra measurement in the total energy range of En=0.01-17 MeV. The group structure used for HPC is 40 or 200 group per decade (gpd). The group structure used for stilbene is the constant energy step in selected energy regions. HPCs were of 4cm diameter and of 100, 400 and 1000 kPa pressure. The dimension of stilbene was of diameter 3x1cm.

Gamma ray spectrometry

Both of the gamma-filed components were measured contemporary. The first one is the primary gamma spectrum of the Cf-252 source attenuated by the nickel sphere, the second one is the secondary gamma of the thermal neutron capture and fast neutron inelastic scattering on the nickel sphere. Both of them were measured by coaxial HPGe-detector (Canberra). The used cylindrical HPGe-crystal was of a diameter 44 mm and of the length 36 mm, FWHM≈3keV (1333 keV), energy region Eg=0.1-10.5 MeV per 8192 channels.

The energy calibration in the whole energy region was made by isotopic point-sources of Co-60, Ba-133 and Cs-137 and by well known distinct energy peaks in the gamma spectrum (H-1, Fe-56, Ni-58, etc.) of the neutron capture.

The efficiency calibration was made by the same isotopic point-sources mentioned above for several axial source-detector distances and for the energy region from 80 keV to 1400 keV. Measured spectra were analyzed by Genie-3.1 Canberra software.

Because of the possible HPGe crystal damage by the higher neutron fluence, the gamma spectra acquisition was not possible for a long time. Therefore some of the gamma spectrum peaks have not sufficiently good statistics. The FWHM parameter was checked periodically for possible detector damage determination.

Calculation

The calculations were performed using Monte-Carlo program MCNP-4C. As for geometry description, a simplified model [6] was used, which substitutes assembly elements with concentric spherical shells around the source. Also, the detector is represented by a 1 cm thick spherical shell with radius equal to the real detector-source distance.

The energy bin structure of resulting tallies was chosen to be logarithmic, either with 40 or with 200 groups per decade. Photon tallies start at 0.001 MeV and end at 12.59 MeV, while neutron tallies range from 1E-10 MeV to 22.39 MeV. However, only 10 groups per decade scale are used up to 0.001 MeV. The evaluated nuclear data files were processed using NJOY-99.115.

Normalisation and smoothing of results

The result of spectra calculation and measurement $\phi(E)$ [$cm^{-2}s^{-1}MeV^{-1}$] is normalized in the following way:

$$\phi_{norm}(E) = \phi(E) \times (4\pi \times R^2/Q) \ , \qquad (1)$$

where R [cm] is the distance between detector and neutron source (centre to centre) and Q[s^{-1}] is the neutron source emission.

For neutron leakage spectra the quantity depicted in the figures has the following form and dimension:

$$E\phi(E)4\pi R^2/Q \ [1] \qquad (2)$$

The calculated neutron spectra were smoothed by Gaussian with constant percentage resolution Δ of FWHM:

Δ=13% for 40 gpd and Δ=4% for 200 gpd.

The so-called absolute efficiency $\varepsilon(E)$ for specific energy gamma E [MeV] was determined as the mean value from the detector response measurements at several gamma source-detector distances r:

$$\varepsilon(E) = \nu_r(E) / \phi_r(E) = \nu_r(E) / (A \times y(E)/4\pi \times r^2) \qquad (3)$$

where $\nu_r(E)$ is the count rate of calibration source at the distance r, $\phi_r(E)$ is the flux density at the distance r [cm], **y**(E) is the decay yield and A [Bq] is the activity of radionuclide which is the source of energy E.

The number of the gamma-rays (photons) G(E) of given energy E emitted from the Ni-sphere for the unit neutron source (*i.e.* falling on 1 neutron emitted from the neutron source) is then:

$$G(E) = (\nu_R(E) / \varepsilon(E)) \times (4\pi \times R^2/Q) \ [1], \qquad (4)$$

where $\nu_R(E)$ is the count rate of leakage gamma when the distance between detector and neutron source placed in the sphere is R [cm]. The quantity G(E) of dimension one is compared with the calculated one thereinafter (Table 2).

Uncertainties

MCNP code gives only uncertainties which are smaller than 5% for En<6 MeV, 40 gpd and 10^8 histories. Statistical uncertainties of H-detector measurements are calculated and represent the values about 3% for spectrum maximum for **NI DIA50, R100** assembly and about 1% for **NI DIA50, R28** assembly. These uncertainties were assessed for 40 gpd.

Statistical uncertainties of integral values are adequately calculated. Uncertainties based on evaluation methodology of spectra measured by hydrogen proportional counters (like energy calibration etc.) are estimated by authors to be approx. 3-7% for energy range 0.01-0.15 MeV and 1-2% for energy range 0.15-1 MeV.

Uncertainties of stilbene measurements are estimated by authors to be 7-15% for energy range 1-17 MeV.

Statistical uncertainties of HPGe detector measurements of listed energy peaks are less than 7%. The uncertainties of the *absolute efficiency* ε values are less than 4%. The distance R and the source emission Q uncertainties were also taken into account in the G-quantity uncertainty calculation.

Estimation of other existing uncertainties (as well as of the source emission, efficiency of detectors etc.) is out of this article scope.

Results of measurement and calculations

Five experimental measurements performed are presented in the Table 1.

Table 1: Measurements on nickel sphere by different types of detectors: HPC, stilbene and HPGe

NI DIA50, R100 - distant measurement			
No.	**Detector**	**Irradiation**	**Note**
1	HPC Stilbene	Neutrons Neutrons	Binding energy 1.3 MeV. Figure 2
2	Stilbene	Gamma	Figure 7
3	HPGe	Gamma	Figure 8
NI DIA50, R28 – measurement on the surface			
No.	**Detector**	**Irradiation**	**Note**
4	HPC	Neutrons	Figure 3
5	HPGe	Gamma	

Neutron spectra

Comparisons of measured and calculated neutron spectra are presented in the Figures 2–6.

Figure 2: Assembly: NI DIA50, R100, 40gpd. Meas. by HPC and for Eg>1.5MeV stilbene (thick), calc. by ENDF/B-VII.0 smooth. Δ=13% (thin)

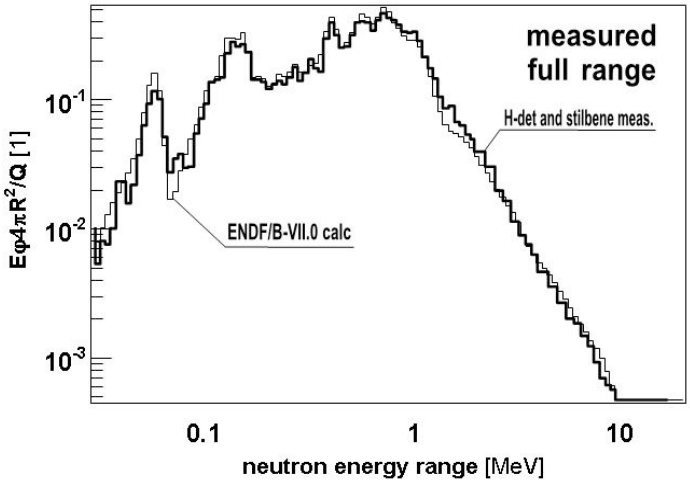

Figure 3: Assembly: NI DIA50, R28, 200 gpd, measurement by HPC (thick), calculation by ENDF/B-VII.0 smooth. Δ=4% (thin)

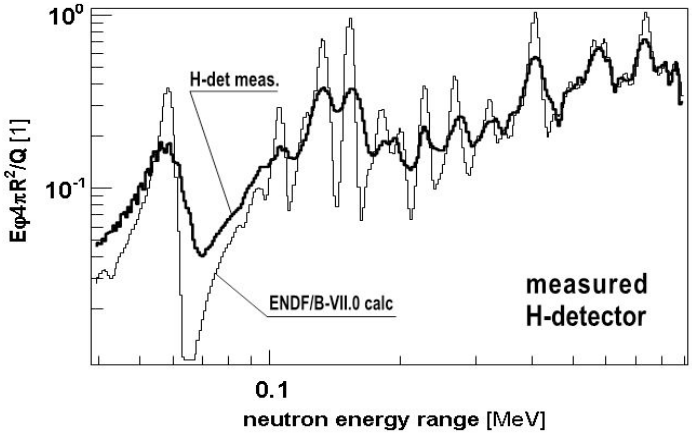

**Figure 4: Assembly: NI DIA50, R100, 40 gpd.
Calc. by JENDL-3.3 (thick), ENDF/B-VII.0 (thin).**

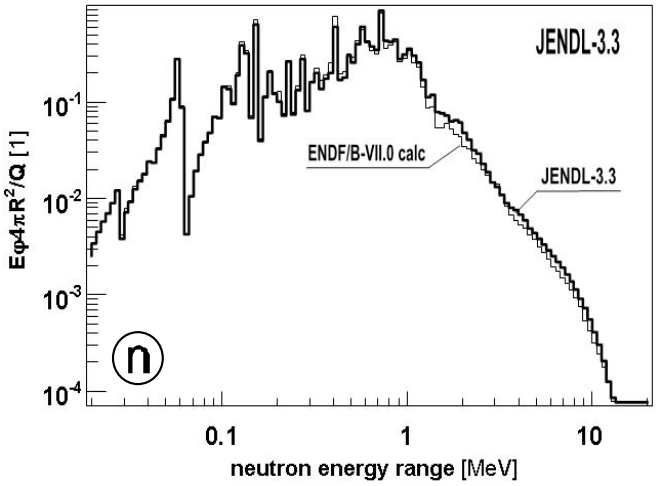

**Figure 5: Assembly: NI DIA50, R100, 40 gpd.
Calc. by JEFF-3.1. (thick), ENDF/B-VII.0 (thin).**

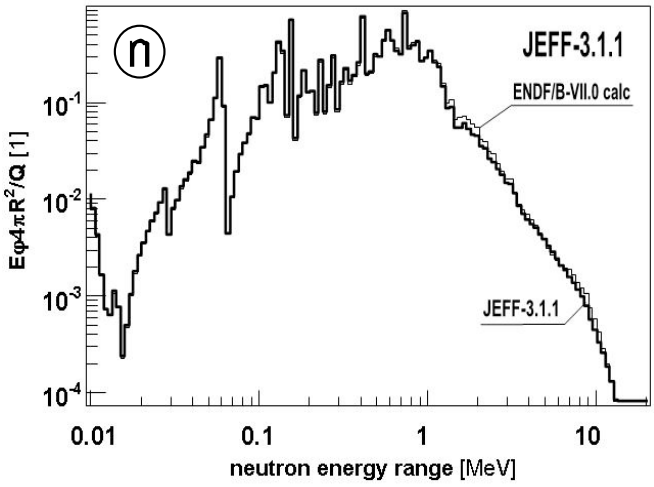

**Figure 6: Assembly: NI DIA50, R100, 40 gpd.
Calc. by TENDL-2009 (thick), ENDF/B-VII.0 (thin).**

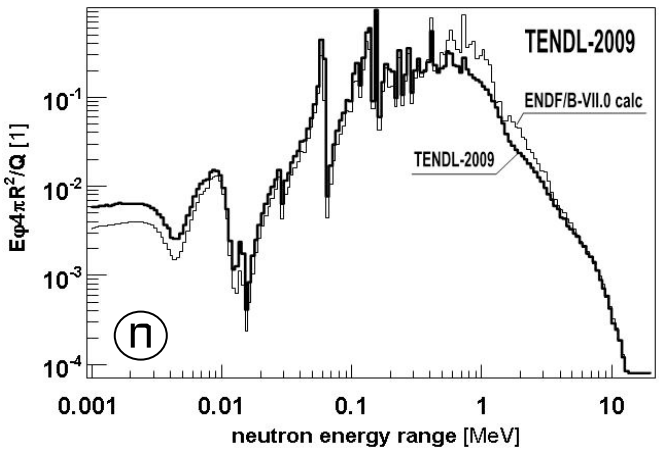

Gamma spectra

Comparisons of measured and calculated gamma spectra are presented in the Figures 7–10. The gamma spectra measured by HPGe were divided in two parts:

a) **Qualitative** – the comparison of the measured and calculated gamma lines (peaks) presence (identification) in the spectrum. The measurement results for this case are in the Figure 8.

b) **Quantitative** – the comparison of the quantity G for specific energy lines: 511 keV, 1333 keV, 1454 keV. The results are in the Table 2 and in the Figure 11 (left R=28cm, right R=100 cm).

Figure 7: Assembly: NI DIA50, R100. Calc. by ENDF/B-VII.0. (thin), meas. by stilbene (thick).

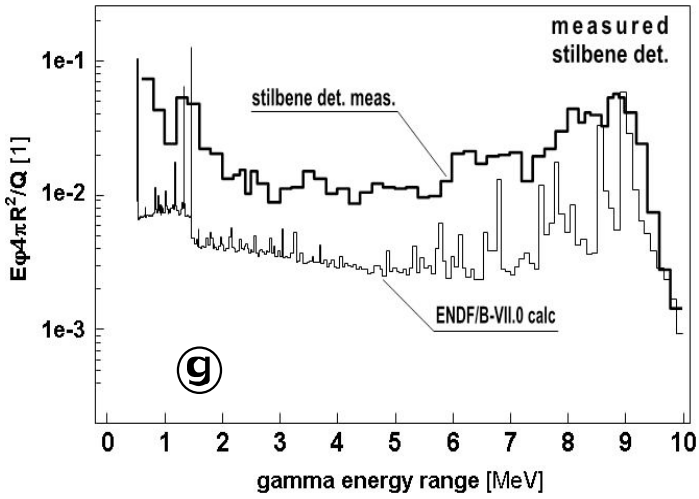

Figure 8: Assembly: NI DIA50, R100. Calc. by ENDF/B-VII.0. (thin), meas. by HPGe (thick)

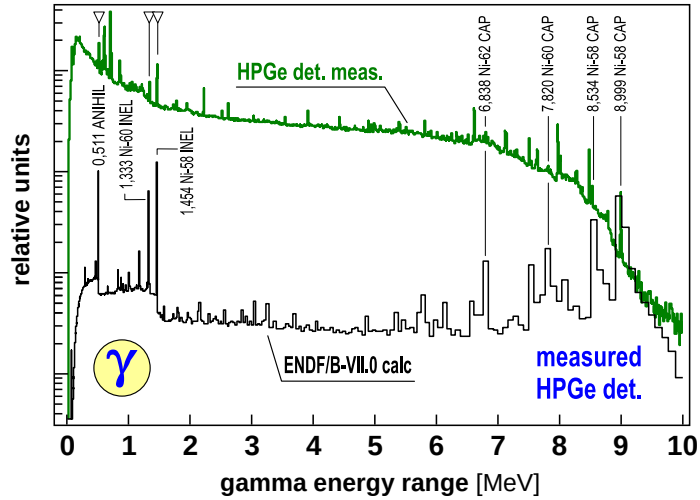

Figure 9: Assembly: NI DIA50, R100, 200 gpd, JENDL-3.0 (thick), ENDF/B-VII.0 (thin)

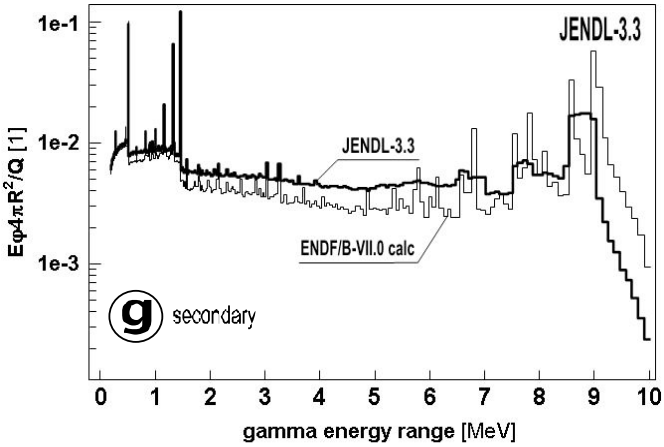

Figure 10: Assembly: NI DIA50, R100, 200 gpd, TENDL-2009 (thick), ENDF/B-VII.0 (thin)

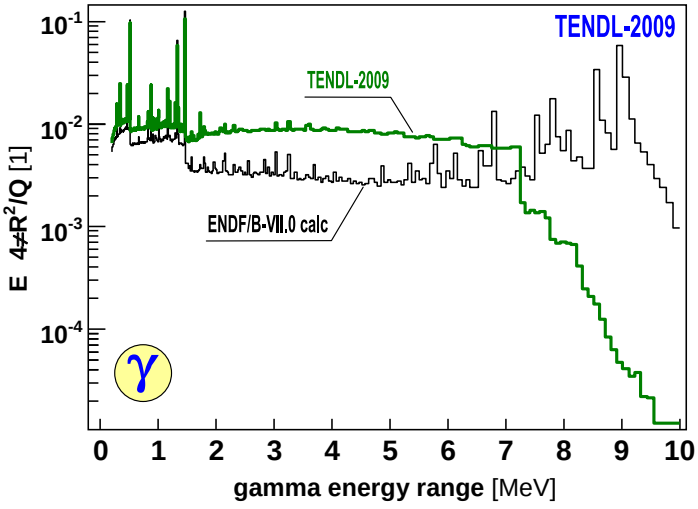

Table 2: a) Quantitative comparison of the quantity G. The G quantity comparison of the HPGe measurement and of the MCNP calculations. G = (flux density x 4pR2/Q) of the gamma-lines of certain energy emitted from the Ni- spherical assembly NI DIA50 R28 and NI DIA50 R100.

Assembly	NI DIA50 R28 (R=28 cm)		
E_g(keV)	**511**	**1333**	**1454**
MEAS	1.34E-03	9.00E-04	1.68E-03
uncer. [%)	3.9	3.6	3.6
ENDF/BVII.0	1.46E-03	8.46E-04	1.79E-03
JEFF3.1.1	1.46E-03	9.35E-04	1.74E-03
JENDL-3.3	1.35E-03	8.39E-04	1.72E-03
JENDL-4.0	1.34E-03	8.24E-04	1.71E-03
TENDL-2008	8.03E-04	8.91 E-04	1.42E-03
TENDL-2009	1.35E-03	8.08E-04	1.43E-03
CENDL-3.1	1.33E-03	8.78E-04	1.68E-03
Assembly	**NI DIA50 R100 (R=100 cm)**		
E_g(keV)	**511**	**1333**	**1454**
MEAS	1.08E-03	7.81E-04	1.50E-03
uncer. [%)	4.6	5.8	3.3
ENDF/BVII.0	1.11E-03	6.50E-04	1.38E-03
JEFF3.1.1	1.10E-03	7.19E-04	1.34E-03
JENDL-3.3	1.02E-03	6.45E-04	1.33E-03
JENDL-4.0	1.02E-03	6.63E-04	1.32E-03
TENDL-2008	6.09E-04	6.91E-04	1.10E-04
TENDL-2009	1.03E-03	6.26E-04	1.11 E-03
CENDL-3.1	1.01 E-03	6.74E-04	1.30E-03

Table 2: b) Quantitative comparison of the quantity G, calculation/experiment–1, in %

Assembly	NI DIA50 R28 (R=28 cm)		
E_g(keV)	**511**	**1333**	**1454**
M EAS	0.00	0.00	0.00
ENDF/BVII.0	8.96	-6.00	6.55
JEFF3.1.1	8.96	3.89	3.57
JENDL-3.3	0.75	-6.78	2.38
JENDL-4.0	0.00	-8.44	1.79
TENDL-2008	-40.07	-1.00	-15.48
TENDL-2009	0.75	-10.22	-14.88
CENDL-3.1	-0.75	-2.44	0.00
Assembly	**NI DIA50 R100 (R=100 cm)**		
E_g(keV)	**511**	**1333**	**1454**
M EAS	0.00	0.00	0.00
ENDF/BVII.0	2.78	-16.77	-8.00
JEFF3.1.1	1.85	-7.94	-10.67
JENDL-3.3	-5.56	-17.41	-11.33
JENDL-4.0	-5.56	-15.11	-12.00
TENDL-2008	-43.61	-11.52	-92.67
TENDL-2009	-4.63	-19.85	-26.00
CENDL-3.1	-6.48	-13.70	-13.33

Figure 11: Quantitative comparison of G from Table 1 (left R=28cm, right R=100 cm). Values are related to the measurement with HPGe spectrometer.

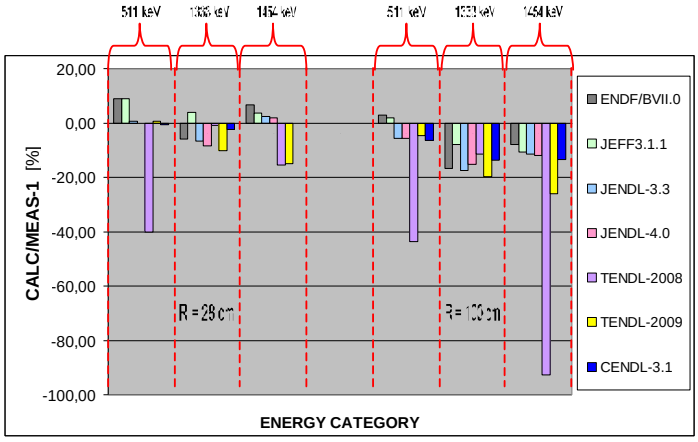

Results in the tables and figures mentioned above show differences between distances R=28 cm and R=100 cm.

Distance R=28 cm

The JEFF-3.1.1 data overestimated slightly the experiments for Eg=511 keV, 1332 and 1454 keV. The ENDF/B-VII.0 data overestimated slightly the experiments for Eg=511 keV and 1454 keV, and underestimated slightly the experiments for Eg=1333 keV. All others libraries underestimated the measured data.

Distance R=100 cm.

The JEFF-3.1.1 data and ENDF/B-VII.0 data overestimated slightly the experiments for Eg=511 keV. For Eg=1333 and 1454 keV all libraries underestimated the measured data up to 25%.

Eg < 2 MeV - all the libraries used for MCNP have acceptable mutual agreement.

Eg > 7 MeV – TENDL-2009 strongly underestimate ENDF/B-VI spectrum.

Eg = 2-6 MeV - the big differences (factor 2-3) between libraries (Figure 13 and Table 4).

Final comparison of measured and calculated spectra

The final comparison of measured and calculated integral neutron spectra is presented in the Table 3 and in the Figure 12, The final comparison of measured and calculated integral gamma-ray spectra is presented in the Table 4 and in the Figure 13.

Table 3: Assembly NI DIA50, R100; 40gpd, HPC and stilbene measurement – differences between calc. relative to meas. in %. Energy range is in MeV.

	Energy range		Libraries used for MCNP calculation			
No.	from	to	ENDF	JENDL	JEFF	TENDL
0	0.10	10.00	3.83	3.65	4.05	-10.97
1	0.10	0.20	14.40	6.74	10.41	60.61
2	0.20	0.35	6.00	-2.19	0.27	31.99
3	0.35	0.45	13.53	-7.80	6.73	-0.52
4	0.45	0.90	5.31	8.93	7.51	-40.01
5	0.90	1.40	-12.74	-1.36	-8.42	-54.78
6	1.40	3.00	-20.20	3.63	-4.24	-48.02
7	3.00	5.00	8.29	20.72	16.17	-12.29
8	5.00	10.00	16.99	44.66	24.41	14.42

Figure 12: Assembly: NI DIA50, R100, 40 gpd. Measurement by HPC and stilbene. Comparison of calc. relative to meas. (Table 3).

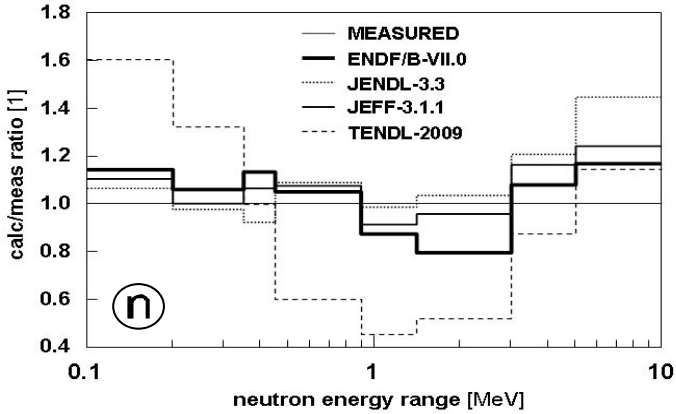

Table 4: The comparison of the libraries for chosen gamma-ray energy ranges. The results are related to the ENDF/B-VII.0.

Energy range [MeV]	ENDF/BVII.0	JEFF3.1.1	JENDL-3.3	JENDL-4.0	TENDL-2008	TENDL-2009	CENDL-3.1
0.1-10.5	1	0.998	1.097	1.098	1.288	1.339	1.210
0.1-0.4	1	1.002	1.074	1.075	1.336	1.268	1.181
0.4-1	1	1.002	1.107	1.109	1.365	1.299	1.164
1-2	1	1.009	1.136	1.135	1.489	1.354	1.255
2-6	1	0.948	1.418	1.423	1.982	2.619	1.926
6-7	1	0.994	1.213	1.217	0.371	1.554	1.273
7-8	1	1.061	0.839	0.834	0.084	0.394	1.084
8-9.3	1	0.992	0.650	0.652	0.005	0.016	0.319
9.3-10.5	1	1.040	0.247	0.248	1.000E-7	0.006	0.131

Figure 13: The comparison of the libraries for chosen gamma-ray energy ranges (Table 4)

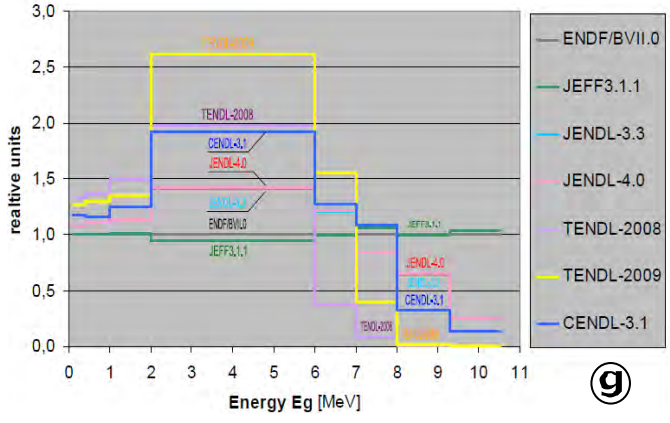

Conclusion

Based on measured and calculated spectra described in the Tables 3 and 4 and in the Figures 12 and 13 we can state the following:

Neutrons:

The graph in the Figure 12 compares calculations using different libraries with measurement (see also Table 3):

En = 0.1-0.9 MeV - calculations overestimate measurement from 5 to 15%

En = 0.9-3 MeV - calculations underestimate measurement from 10 to 20 %

En = 3-10 MeV calculations overestimate measurement. JENDL overestimate measurement from 20 – 40%.

The calculation with TENDL differs remarkable from other libraries (from -50 to +60%).

Gamma:

Measurements with HPGe detector confirm existence of the expected main gamma lines in calculated spectrum for all libraries used in energy range 0.1-10 MeV except of TENDL-2008 and TENDL-2009 libraries, which strongly underestimate measured spectrum for Eg > 7 MeV.

The calculated values for the chosen gamma lines 511, 1333 and 1454 keV differ no more than 20% from experiments excluding the TENDL-2008 (Figure 11 and Table 2).

Acknowledgements

This work was prepared under project No. 1H-PK2/05 of Ministry of Trade and Industry of the Czech Republic and under the project of the Research Centre Rez Ltd. of the Czech Republic.

References

[1] Jansky, B., *et al.*, "Neutron Spectra Measurement and Calculations Using Different Data Libraries in Iron Benchmark Assembly", *Proc. of the CANDIDE – NEMEA-4 Workshop on Neutron measurements, evaluations and applications*, October 2007, Prague, Czech Republic, Report EUR 23235 EN-2008, p. 79 (2008).

[2] Jansky, B., *et al.*, "Neutron and Gamma Spectra Measurement and Calculations Using Different Data Libraries on Nickel Benchmark Assembly", Proc. of the International Conference on Nuclear Data for Science and Technology, Jeju Island, Korea (2010), forthcoming.

[3] Jansky, B., *et al.*, *Neutron Spectra Measurements and Calculations Using Different Data Libraries on Nickel Benchmark Assembly*, Report JEF/DOC-1296, JEFF Project, OECD/NEA Data Bank (2009).

[4] Jansky, B., *et al.*, "Neutron and gamma leakage spectra measurements and calculations in pure iron benchmark assembly with Cf-252 neutron source", *Proc. Int. Conf. on Nuclear Data for Science and Technology ND 2001*, Tsukuba, Ibaraki, Japan, 2001, *Journal of Nuclear Science and Technology*, Suppl. 2, August (2002).

[5] Kolevatov, Yu.I., V.P. Semenov, L.A. Trykov, *Neutron and gamma spectrometry in radiation physics*, Energoatomizdat, Moscow, Russia, (in Russian) (1990).

[6] Jansky, B., P. Otopal, E. Novak, *Data for calculation of the neutron and gamma leakage spectra from iron and water spheres with Cf-252 neutron source in centre*, NRI report UJV-11506, NRI Rez (2000).

The 2010 compilation of SINBAD: quality assessment of the fusion shielding benchmarks

A. Milocco, I. Kodeli, A. Trkov
Jožef Stefan Institut, Ljubljana, Slovenia

Abstract

SINBAD, the Shielding INtegral Benchmark Archive Database, includes a section with the integral experiments relevant for fusion applications. International facilities (such as OKTAVIAN, FNG, TUD, FNS) contributed neutron and gamma spectra measurements with pulse height or time-of-flight detectors as well as integral measurements using activation foils, fission chambers, thermo-luminescent detectors and dosimeters. A systematic revision of the SINBAD database has been undertaken recently in order to assess, and where possible improve, the quality of the available experimental information. A particular attention was devoted to the complete and consistent evaluation of the experimental uncertainties, since this information is essential for the proper exploitation of the measured data. The revision is expected to facilitate the use of the database and to provide guidance for the selection of experiments suitable for the nuclear data evaluators. The main output of this work is the release of the new more comprehensive and useful SINBAD compilations of the above experiments through the NEA Data Bank.

Introduction

The OECD/NEA Data Bank and ORNL/RSICC joined their expertise in 1996 to produce and maintain SINBAD, the Shielding INtegral Benchmark Archive Database [1]. The 'fusion neutronics section' of the database includes the benchmark information on integral experiments relevant for fusion applications. The material assemblies are irradiated in intense fields of ~ 14 MeV neutrons, produced from Deuteron–Tritium (D–T) reactions. The experimental information available in SINBAD is the object of the recent revision of the database. The quality of any integral experiment is assessed with reference to their completeness, consistency and usefulness for the nuclear data validation. The virtues and the shortcomings are pointed out and the benchmark is classified accordingly. This quality review is expected to facilitate the use of the database and to provide guidance for the selection of experiments suitable for the validation of particular nuclear data or numerical methods. As the first stage, the benchmark experiments performed at the OKTAVIAN, FNG, FNS and TUD facilities were considered in this exercise:

Table 1: Representation of the SINBAD experiments based on the materials

Materials	Experimental data
W	OKTAVIAN neutron/gamma leakage spectra FNS neutron/gamma spectra and reaction rates FNG activation rates and FNG/TUD neutron/gamma spectra
Si	OKTAVIAN neutron/gamma leakage spectra (60 and 40 cm shells)
C	FNS neutron/gamma spectra, activation rates, fission rates and heating
SiC	FNG activation rates and FNG/TUD neutron/gamma spectra
V	FNS neutron/gamma spectra, activation rates and heating
Al	OKTAVIAN neutron/gamma leakage spectra
Fe	OKTAVIAN neutron leakage spectrum TUD neutron leakage spectrum 'FNS neutron streaming (spectra and activation rates)'
Ni	OKTAVIAN neutron leakage spectrum
Stainless Steel	FNG-SS Shield (activation rates)
Stainless Steel + Perspex	FNG activation rates, dose rate and heating
Stainless Steel + Perspex+ Polyethylene + Cu	FNG activation rates and heating FNG/TUD neutron/gamma spectra FNG streaming (activation rates, heating)
O	FNS neutron leakage spectrum
Air	'FNS sky-shine (dose rate and gamma spectrum)'

SINBAD includes neutron/gamma spectra and integral measurements using activation foils, fission chambers, thermo-luminescent detectors and dosimeters. The integral data can be used to validate the primary standards and to crosscheck neutron spectra. They are in general more reliable, accurate and precise than the spectra measurements, but less informative. The FNG/TUD experiments are performed at the same experimental set–up as the FNG ones, only that in the first the neutron/gamma spectra were measured, and in the second the integral quantities. The FNS sky-shine, the FNS Dogleg Duct Streaming and FNG-ITER Neutron Streaming experiments are of particular interest because they address the sky–shine effect and the streaming through the ducts. As such, they are used for the validation of the computational methods.

The major purpose of the SINBAD integral experiments is the validation of modern nuclear data evaluations. It can be reasonably assumed that the benchmark can be useful for the validation and/or improvement of the modern nuclear data evaluations (or methods) only if the effect of the experimental uncertainties is comparable, or lower, than the uncertainties due to nuclear data (or methods). The target accuracies of the modern nuclear data evaluations become more and more demanding and depend on the material and its application. For this reason, the criteria to rank an integral shielding experiment as of benchmark quality are not always easy to define.

In the present review, the experimental information is addresses in as many details as possible and reasonable. The next section focuses on the geometry and material specifications for the assembly of the sample, the experimental room and the detectors. Then, the source specifications are addressed, checking the completeness and consistency of the information provided by simulating the neutron source. A section enlightens the experimental methods employed for the measurements. Namely, the extent is assessed to which the analyst can reproduce the experimental data reduction and processing techniques. In the conclusions, a short note is finally issued on the quality of the experiment presented in the list above. The main outcome of this work is the release of the new more comprehensive and useful SINBAD compilations of the above experiments through the NEA Data Bank.

Geometry and materials

The realistic modelling of the experiment depends on the precise quantitative specification of the geometry and composition of any experimental item. The geometry specifications of an experimental component are considered complete when all relevant dimensions are specified with a numerical value (besides the usual tolerances in the design). The material specifications rely on the definition of composition and density.

The fine reduction of the experimental set-up into the minor items, whose effect cannot be reasonably neglected, is hereby addressed.

Samples

Avoiding approximations in the modelling of the geometry and in the composition of the material assembly is a major requirement for the experiment to be of benchmark quality. The experimental specifications of the test samples are generally complete.

An example of high quality experimental information is represented by the specification of the SS-316 benchmark for the FNG ITER streaming activation measurements. For this experiment, a reference is included in SINBAD, which provides both producer specifications and the tests performed at ENEA on the chemical composition of the bulk material. Such thorough specifications are not usually available.

So far it has been common practice to provide the experimental information (without further testing) in the reports produced at the experimental facility and the benchmark information in the computational models. Cases, where the experimental specifications are available only in the computational models are of concern because the independent checking of the specifications cannot be achieved, the benchmark information cannot be upgraded and the current computer code input files may become unusable in the future. This drawback is found for many FNG/TUD experiments, as well as for the FNS Oxygen and Dogleg Duct experiments.

The quantification of the impurities of the bulk materials may be uncertain (such as the boron concentration in the FNG SiC benchmark, affecting the $^{197}Au(n,\gamma)^{198}Au$ reaction rates) or lacking (*e.g.* for the OKTAVIAN Si experiments, but not likely to affect the measured spectra).

Minor items of the sample assembly can be the stands or other supporting structures. For the FNS V experiment in particular, the Al grid is not clearly specified. The outcome of the sensitivity studies on the supporting Al components is that their effect is negligible.

Experimental hall

The specifications of the OKTAVIAN experimental room are of intermediate quality because some guessing based on common sense is required for its modelling. For instance, the material composition of the walls, which may be important for the interpretation of the neutron leakage spectra, is not provided. The geometry of the room walls can be inferred from the room layouts, which are not very reliable due to scaling factors or image resolution. A new figure is included in SINBAD, which was temporarily available on the Web (Figure 1). The red and the blue lines represent the measuring lines for the Ni and Fe experiments (forward direction) and for the Si, Al and W experiments (55° direction).

The most comprehensive description of the FNS target room 1 is provided for the sky–shine experiment. A brief description and detailed vertical layout of the room are available (Figure 2). This information can be used to model the experimental room for all the other FNS experiments except for the Fe streaming experiment, whose source is located in the adjacent room 2. A discrepancy remains concerning the distance of the source from the west wall. For Graphite experiment, it is said to be 5.5 m and for sky–shine experiment 2.75. Since the beam line was not likely to be modified, the first specification seems more reliable.

A model of the walls at the FNG facility is included in the computational models.

The TUD Fe experiment does not provide the experimental information of the experimental hall, but the method to calculate the background effect is described.

Figure 1: OKTAVIAN room layout

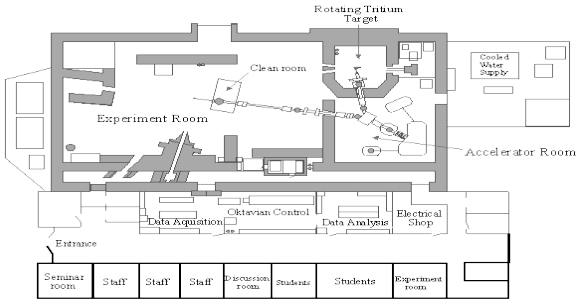

Figure 2: FNS room layout (room 1)

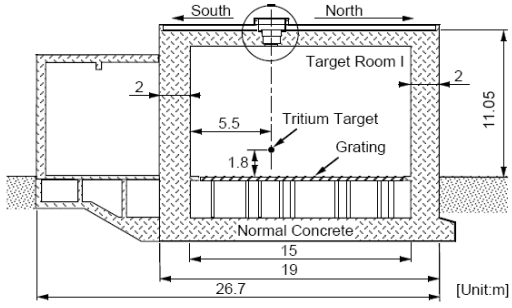

Detectors

The realistic modelling of the detector system for the neutron leakage spectra measurements requires the specification of the collimator/pre-collimator and detector housing. The experimental description of the neutron detector system is ranked as of intermediate quality for the forward line OKTAVIAN experiments and of benchmark quality for the OKTAVIAN 55° detection line. In the latter case, the Figure 3 is found in literature [2] and is included in the new SINBAD compilation because it describes the experimental set–up much better.

Only the O experiment involves a similar detector system at FNS, which is roughly described. The higher order effects due to neutron scattering in the detector system can be anyway neglected because of the major uncertainties on the experimental method (see 'measurements' section).

The gamma leakage measurements performed at the OKTAVIAN 55° line can be approximately modelled. The model is based on Figure 4, which is retrieved from the literature [3] and is now available in SINBAD. The geometry and material specifications of this detector are considered of intermediate quality, especially concerning the material specifications.

The FNS and FNG/TUD neutron spectra measurements are performed in the MeV region with NE213 detectors placed inside the sample. Experimental information is usually available on their material composition, geometry, positioning and experimental channel in the sample assemblies. In the FNS W and V cases, the neutron spectra are measured also at lower energies by Proton Recoil Counters (keV energy region) or Slowing Down Method (eV energy region). Even if there is enough experimental information to model any set of measurements, a practical solution is to develop a single detector model to be used for any measurement. A proper choice of the approximations introduced in the benchmark models is illustrated in Figure 5. The realistic NE213 detector is represented by a sphere filled with a C-H mixture. The NE213 detector model distorts the flux in the keV region, as can be seen by comparison with the flux in the same sphere but setting the material density to ~ 0, which is more realistic for the Proton Recoil Counters filled with gas. The flux calculated across a surface at the same position is a good compromise for both measurements, beside statistical fluctuations.

In the FNG/TUD experiments, the gamma–ray fluxes in the range E>0.2 MeV are simultaneously measured using the NE213 scintillator as for the neutron spectra.

The gamma ray spectrometer BC237 is used in the FNS W and V experiments. The geometry and the material composition of the spectrometer are completely defined, but some approximation remains concerning the experimental channels.

For the FNS activation experiments, the geometry of the foils is specified. The natural composition and density of any foil can be assumed. The positions of the foils inside the assembly are approximately given (without specifying the uncertainty). In similar experiments, more foils are often activated at the same time. The exact sequence of the foils arrangement can be important experimental information for some reaction rates because of the mutual shielding effects and large flux gradients. Moreover, the possible supports of the foils are not described. The effect of the realistic modelling of the activation foils can be seen by comparing the reaction rates calculated with different detector models. The detector tallies are approximate with a surface flux ('simple' in Figure 6) or realistic because the Nb, Al and In foils are explicitly modelled. The effect of the detector modelling can be quite important, so the experimental specification of the foils stacking is quite relevant.

For the FNG activation experiments, the experimental information is considered complete and precise.

The experimental information in the FNS C case is not sufficient for simulating the gamma ray heating measurements, mainly because little information is available on the detectors (dimensions, composition). It is feasible to simulate the TLD measurements in the W and V assemblies at FNS.

The material composition, geometry and positioning of the TLDs are specified for the FNG experiments. A model of the walls at the FNG facility in included in the computational models.

Figure 3: Oktavian 55° neutron detector system

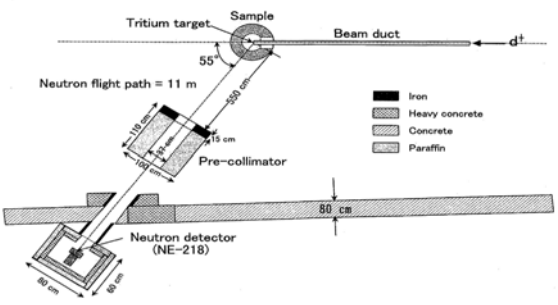

Figure 4: Oktavian 55° gamma detector system

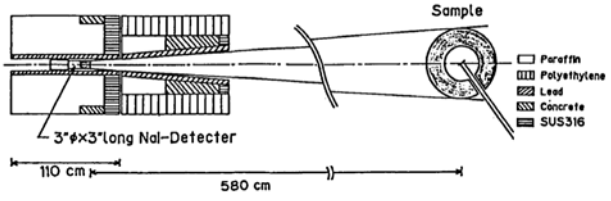

Figure 5: Effect of the approximations introduced in the detector benchmark models

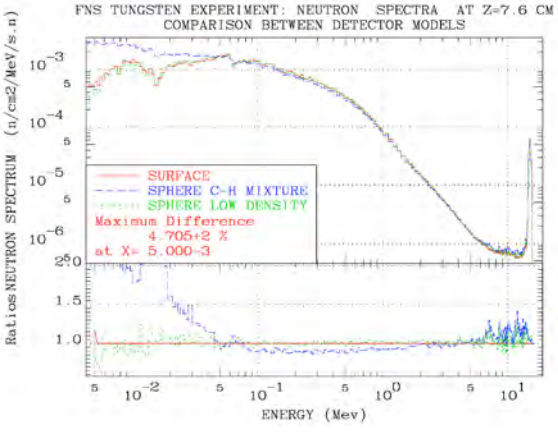

Figure 6: Effect of the approximations in the FNS activation foils modelling

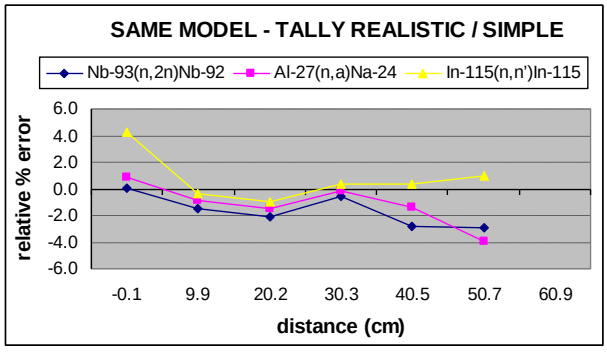

Source

The neutron source term determines the ~ 14 MeV elastic peaks, which in turn validates the elastic cross-section at these energies. In the inelastic region (from ~ 7 to ~ 14 MeV), the interactions of the source neutrons with structural components affect the spectra measurements, especially if the sample does not shield too much [4]. The use of the experimental source spectrum in the simulation of the integral experiments is quite common, but the approach is an approximation (especially in the case of neutron leakage spectra measurements) because the experimental configuration of the source measurements is different from the set-up with the sphere in place. To reduce the approximations it is advisable to simulate the neutron source too. This can be done including in the computational model as much experimental information as possible, but its consistency and completeness needs to be assessed.

FNG and FNG/TUD

The FNG source specifications rely on a routine, which models the D–T source at FNG. A set of subroutines are provided in SINBAD to compile with the MCNP4B, MCNPX or MCNP5 source codes [5]. The version originally developed at FNG (labelled 'MCNP4B') is now considered obsolete. For the occasion of this SINBAD revision, the D–T source routine has been refined and upgraded for the most recent releases of the MCNP family of codes. The current D–T source model features the deuteron slowing down inside the Titanium–Tritium target and the D–T reactions, including realistically the anisotropy effects and the relativistic kinematics. The source routine requires the use of the RDUM card to define the deuteron beam energy, target thickness, T/Ti atomic fraction, beam width, target axis coordinates.

The present MCNP5 simulations of the neutron source spectra make use of the revised D–T source routine (MCNP5 version) and include the source assembly. The specifications for the source assembly are of high quality for the experiments performed at FNG because full details on the ion tube, Ti–T target and cooling system are provided, even if this information is contained in the input files for the MCNP–codes. The comparison between the source spectra calculated with the obsolete and the revised versions are presented in Figure 7 in the forward, perpendicular and backward directions. At 0°, the revised version produces a shifted spectrum due to the introduction of the relativistic kinematics. The revised D–T source routine is hereby validated against bare source measurements with a diamond detector. The experimentalists at FNG provided the raw experimental data, which are the counts per channel of the measurement. The transformation into the energy spectra was performed applying the calibration formula and an energy shift of 5.7 MeV due to the kinematics of the $^{12}C(n,\alpha)^{9}Be$ reaction in the diamond detector. The tails in the measurements below the ~14 MeV peak are due to the incomplete charge collection in the diamond detector. These cannot be reproduced with the MCNP5 model. A 1% FWHM Gaussian broadening was applied to calculated spectrum in the forward direction. The agreement at the 14 MeV peak is fairly good (Figure 8). The major concern is the detector model, which in this case cannot be developed because of the intrinsic limitations of the MCNP5 code.

Figure 7: source spectra simulated with the MCNP-4B and MCNP5 source versions

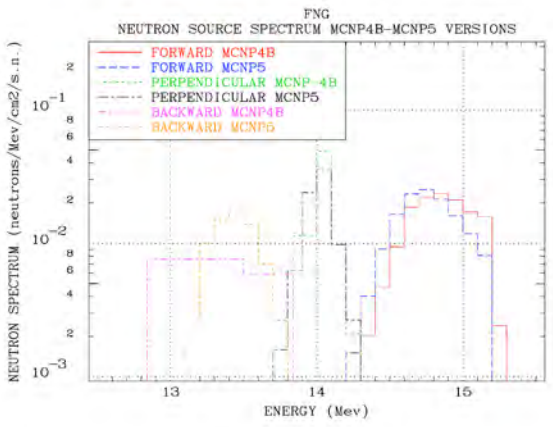

Figure 8: MCNP5 simulation of the source spectrum for the diamond detector experiment

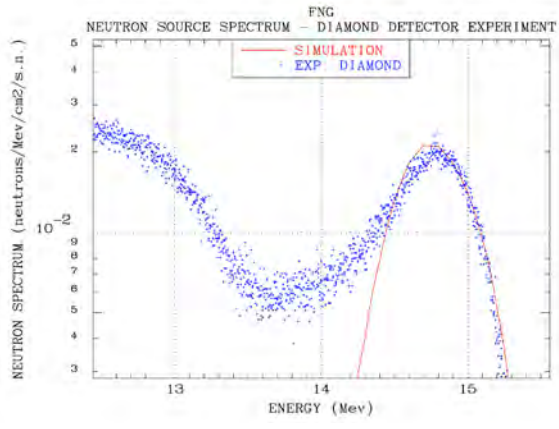

The source specifications for the Fe TUD experiment are contained in the benchmark model. Although the quality of the information is questionable because no measured source spectrum is provided, it can be seen a posteriori that the source specifications work fine at the ~14 MeV peak.

OKTAVIAN

The experimental neutron source spectra, which are recommended for the Si and Al experiments, are quite similar (Figure 9). They differ from the source spectrum specified for the W experiment below 5 MeV (Figure 9), but no explanation was found. These spectra are provided in a coarse energy mesh, which is particularly evident at the 14 MeV peak. The use of these source spectra requires interpolation to a finer energy grid.

The recommended source spectrum for the forward line experiments is the one labelled as 'nickel/iron' in Figure 9. Its statistical uncertainties are not given, which is an important shortcoming.

The D–T source routine (MCNP5 version) described in the previous paragraph is used to simulate the neutron production from the D–T target at the OKTAVIAN facility. The most important input parameter characterising the physics of the D–T reaction is the deuteron energy, which is duly provided for any experiment. Applying some common sense is usually sufficient for overcoming lacking experimental information on the other input parameters.

The theoretical angular distribution of the D–T neutrons is presented in Figure 10 ('D–T kinematics') for the OKTAVIAN deuteron energy. The yields are calculated from the ENDF/B-VII evaluation of the Legendre coefficients. The difference with the yields obtained from the MCNP5 model, which uses the D–T source routine and point detectors in the void ('simulation without source assembly') represents the effect of the Ti–T target thickness. The experimental information on the source assembly of the OKTAVIAN facility is lacking, partial or contradictory. Nevertheless, an approximate model for the source assembly is developed and included in the MCNP5 model. The dip is observed in the angular distribution because of the source assembly (Figure 10). It is not possible to reproduce the experimental yields ('OKTAVIAN specifications') in the backward direction because the flange and cooling system cannot be modelled. It is advisable to take into account the anisotropic effects in the OKTAVIAN experiments because the neutrons start at the centre of the sample assemblies.

For the 55° line experiments, the modelling of the neutron detector system (pre-collimator, collimator, detector housing and detector) is feasible, as previously discussed. The results of the simulation with full experimental set–up are compared with the experimental source spectrum as specified for the Al experiment ('simulation' in Figure 9). The agreement is satisfactory, especially at the ~ 14 MeV peak. The discrepancies between 5 MeV and 10 MeV and below 1 MeV are due to the approximation of experimental method, such as the background subtraction [4]. The experimental

Figure 9: OKTAVIAN experimental neutron source spectra and simulation with a realistic MCNP5 model of the 55° line neutron source

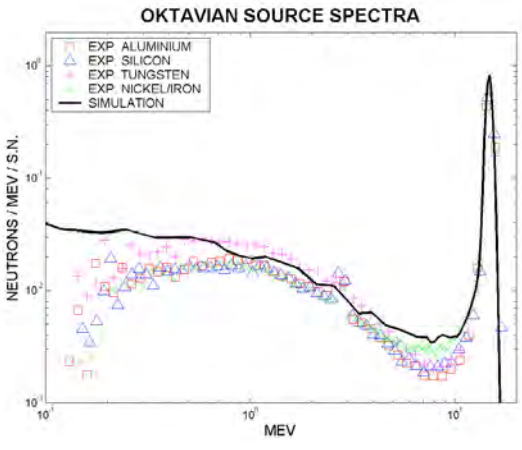

Figure 10: Simulation of the OKTAVIAN specification of the neutron yielding

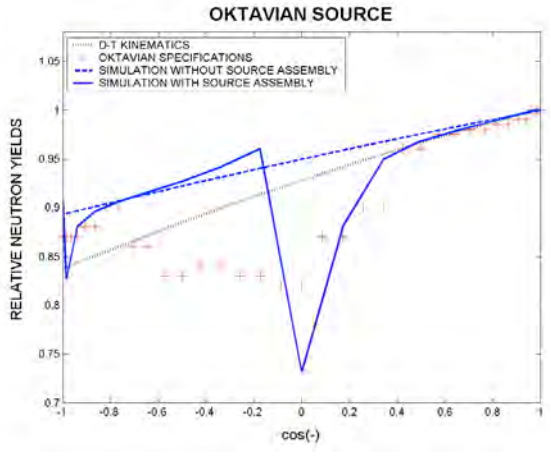

information on these realistic effects, especially at lower energies, represents a major drawback for the experiments performed in the 55° line of the OKTAVIAN facility.

A model of the gamma detector (from the Figure 4) is developed and included in the previous MCNP5 model for the simulation of the gamma source spectrum. The results of the calculations are not satisfactory and are not presented hereby. Thus, extra experimental information is requested on the gamma source measurements.

No simulation is pursued in the Fe and Ni cases because the approximations that would be introduced in the geometry and material composition of the detector system are greater than in the previous case. The use of source anisotropy specifications can be recommended, but the use of the experimental source spectrum requires caution.

FNS

The neutron source spectrum for the C experiment was calculated at FNS. The measured source spectrum is not available in a computer readable format. So far, the agreement between the results of the FNS calculations and the measurements can be ascertained from a figure in [6]. The source spectra specified for the W and V experiments were calculated as well. The discontinuity at about 0.1 MeV is not realistic (Figure 11). The evident difference with the C source spectrum (Figure 11) is due to the modification of target assembly at FNS. The measured neutron source spectrum to be compared with the calculations for the W/V cases is not available. The source spectrum tabulated for the O experiment seems an experimental one because of the elastic peak broadening and the small peak at 3 MeV due to the D–D reactions (Figure 11). It is not explicitly stated to which source assembly the oxygen experiment refers. The source spectrum described here is the recommended one for the analysis of the O experiment. The neutron source spectrum for the sky–shine experiment is completely different from the other source specifications. No information is available about the source measurements or calculations. For the dog–leg duct experiment in room 2, no source spectrum is provided.

The source spectra calculations at FNS rely on a source routine, which was developed thereby. The source routine is partially listed but cannot be anymore used. The D–T source routine described in the previous paragraph is suggested to replace the original one and perform realistic simulations of the source term. The source specifications for the more recent W and V experiments are assessed because in this case the experimental information is sufficient to model the source assembly. An MCNP5 model is developed, which calls the D–T source routine and includes the source assembly and point detectors at different directions. The comparison is presented between the yields as specified for these experiments and as calculated with the new simulation (Figure 12). The results are clearly consistent in the forward directions. The discrepancy in the backward directions is likely to be due to differences between the present and FNS models. The FNS computational models are not available. This difference should not affect the results too much because the FNS set–up foresees samples that are placed in front of the source.

The new simulations of the forward source spectrum are consistent with the FNS specification (Figure 11). The agreement at the 14 MeV peak suggests that the D–T source routine can reasonably replace the original FNS routine. The major differences are noticed from 7 MeV to 11 MeV and below 1 MeV. This could be due to some experimental components, such as the detector system, that are not included in the present simulation. Information on the detector system, used for the specification of the source spectra at FNS is not available.

To summarise, the shortcomings of the source specifications for the FNS experiments are the following:

- The source spectra for the C, W and V experiments come from calculations performed at FNS. For the W and V cases, the details of the original calculations (source routine, source assembly, detector model) and the measured source spectra are not available.
- The source spectrum provided for the O experiment seems to be a measured one, but the details of the measurement are not available.
- In the case of the sky-shine experiment, the simulation of the source term is not feasible because very little information is provided.
- In the case of the dog–leg duct experiment, no source spectrum is provided. The original input files for the MCNP-4B require a source routine, which was developed at FNS and is not anymore available. As last resort, the D–T source model employed in present simulations is recommended.

Figure 11: The FNS neutron source spectra specifications and simulation of the neutron source spectrum for the W and V experiment

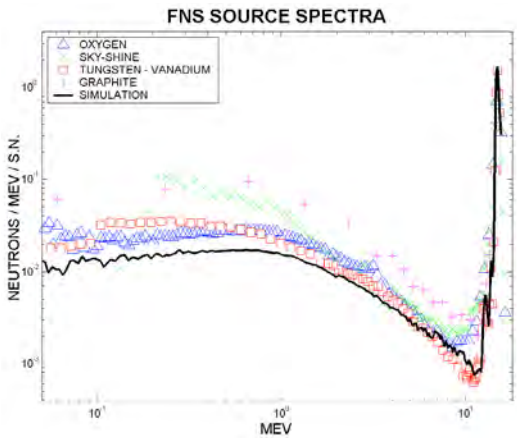

Figure 12: Simulation of the FNS specification of the neutron yielding

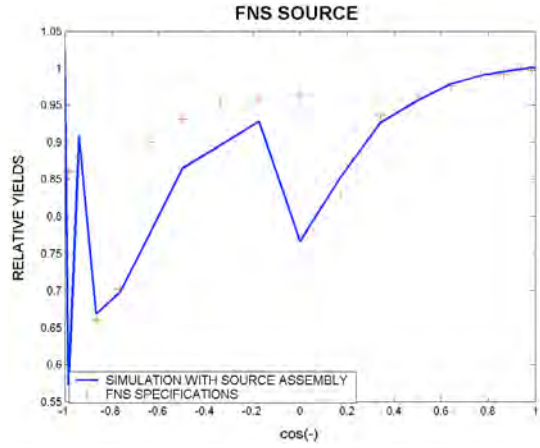

Measurements

The first, obvious requirement for the quality assessment of the measurements is that the experimental data are provided together with the associated uncertainties. The main outcomes of the quality assessment are the following.

- The OKTAVIAN Fe measurements above 4 MeV are affected by large uncertainties, and therefore of very limited use for the modern high–accuracy requests of Fe cross-sections.
- The OKTAVIAN Si-40 cm experimental neutron spectrum is retrieved by digitalisation of Figure 5.3.5 in [7], thus the results of the measurements are approximate and do not include the uncertainties. A table with the approximated results of the measurements is included in the new SINBAD compilation.
- The FNG/TUD W and SiC spectra measurements do not include the point-wise uncertainties. The experimental uncertainties are estimated in energy ranges, which is an approximate approach.
- The FNS sky-shine experimental information does not allow determining the dose because the efficiency function of the detector is lacking.

The spectra measurements provided in SINBAD are the last step of experimental data processing and reduction, which could be reproduced by computational methods if the primary experimental information were available, such as the Time–of–Flight (TOF) or Pulse–Height–Spectra (PHS). In particular, the neutron/gamma spectra are in general considered less reliable than the integral measurements (activation, fission, heating and dose rates) because of the uncertainties introduced in the unfolding procedures or in the transformation from time to energy domain. These techniques are further investigated in the next sections.

TOF measurements

The TOF technique is used for the neutron spectra measurements in all OKTAVIAN, TUD–Fe and FNS–O experiments. The requirements from the experimental information concerning TOF measurements are established with some engineering judgement because guidelines for these experiments have not been produced yet. High quality TOF measurements would provide: 1) TOF spectrum in computer readable format, 2) efficiency function in computer readable format, 3) time and energy uncertainty associated with the detector and the neutron source, 4) time into energy transformation method and parameters, such as time zero or flight path, 5) method for background subtraction.

The SINBAD compilation of the TUD-Fe experiment provides the TOF spectra and the efficiency function in numerical format and an evaluation of the time uncertainty. Thus, the measurements for this experiment are considered of high quality.

For the OKTAVIAN Fe and Ni experiments, the figures representing TOF spectra and efficiency functions are provided, but the representation is not convenient. The components of the time/energy uncertainties are tabulated for the OKTAVIAN forward line experiments. They can be approximately applied to the 55° line experiments.

The description of the experimental method adopted to subtract the background is not found for any experiment, as already observed during the simulation of the OKTAVIAN 55° source spectra.

The specification of the method for transforming the TOF spectra into energy domain spectra is never explicit. The use of some common sense is enough to get consistency with the transformation adopted in the OKTAVIAN experiments. Nevertheless, the following drawbacks are noticed.

In the Fe experiment the transformation is classical, which is an approximation for neutron energies above ~ 10 MeV.

- In the Al experiment, the nominal flight path seems approximate [4].
- Three different methods could be applied for the analysis of the O experiment, which are described in the reports dealing with similar TOF experiments at FNS. These methods require further investigation.

PHS measurements

The pulse height technique is adopted for the neutron spectra measurements by the NE213 detector in the FNS/TUD in situ and streaming experiments and for all the gamma spectra. The measured PHS are not a direct requirement for the quality of the benchmark experiment because of the analytical difficulties in their simulation (*e.g.* with MCNP5). Nevertheless, they are primary experimental information, which is considered valuable for future analyses. In most SINBAD compilations, the PHS are not available. This is acknowledged as a deficiency in the experimental information.

The experimental spectra provided by the TUD team do not include the effect of the detector resolution and thus compare directly with the calculated spectra. The unfolding procedure cannot be assessed since the PHS and the detector resolution function are not available.

For the FNS in situ experiments, the comparison between calculated (Φ_{true}) and measured (Φ_{obs}) spectra requires the application of the detector energy resolution to the calculations. The response function consists of Gauss functions with standard deviations that vary with energy:

$$\Phi_{obs}(E) = \int_0^\infty \frac{1}{\sqrt{2\pi}\,\sigma(E)} \exp\left[-\frac{(E-E')^2}{2\sigma^2(E)}\right] \Phi_{true}(E')dE' \qquad (1)$$

A MATLAB program was developed, which applies Eq. (1) to the calculated spectra (Figure 13). The experimental spectra have an oscillatory structure due to a mismatch between the real detector response function and the one used during the data processing. Nevertheless, it is still possible to recognise the effect of the nuclear data, since a problem in the ENDF/B-VII library is found (Figure 13).

The detector response function for the FNS Fe streaming measurements is not provided.

The detector response functions for the gamma spectra measurements at the OKTAVIAN (W, Al, Si experiments) are not given.

Integral measurements

A set of activation foil measurements are available. These measurements are useful for the validation of the nuclear data evaluation for specific reaction channels. Thus, they are quoted in Table 2.

The activation rate measurements are in general more reliable than spectra measurements and can be used to validate the spectra measurements where both are available. Documents included in SINBAD discuss the coherence between activation and neutron spectra measurements for some FNG/TUD experiments. Both measurements were found to be reasonably consistent in the case of the ITER Bulk Shield experiment. Concerns about the coherence between the spectra and activation measurements are expressed for the SiC experiment. The coherence test is not passed for the ITER Streaming experiment, therefore the respective spectra measurements are not included in SINBAD. For the FNG/TUD W experiment, the consistency is questionable and the integral measurements could be considered more reliable than spectra measurements [8].

Figure 13: Example of application of the detector resolution function to the calculated spectra of the in situ FNS experiments

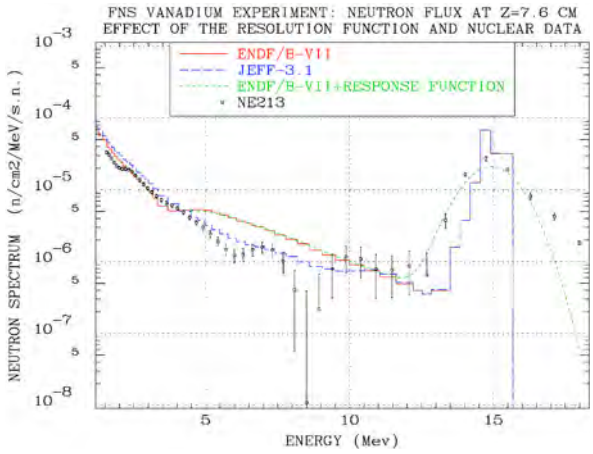

Table 2: Reaction rates measured at FNS and FNG; legend: X = yes (available), – = not available; C = Graphite, W = Tungsten, V = Vanadium, ST = Streaming, SiC = Silicon Carbide, SS = Stainless Steel, BB = Blanket Bulk, DR = Dose Rate

	FNS				FNG					
Reaction	**C**	**W**	**V**	**ST**	**W**	**SiC**	**SS**	**BB**	**ST**	**DR**
$^{27}Al(n,\alpha)^{24}Na$	X	X	X	–	X	X	X	X	X	–
$^{58}Ni(n,2n)^{57}Ni$	X	–	–	–	X	–	X	X	–	X
$^{58}Ni(n,p)^{60}Co$	X	–	–	–	X	X	X	X	X	X
$^{90}Zr(n,2n)^{89}Zr$	X	–	–	–	X	–	–	–	–	–
$^{56}Fe(n,p)^{56}Mn$	–	–	–	–	X	–	X	X	–	–
$^{93}Nb(n,2n)^{92m}Nb$	X	X	X	X	X	X	–	X	X	–
$^{115}In(n,n')^{115m}In$	X	X	X	X	X	–	X	X	–	–
$^{197}Au(n,\gamma)^{198}Au$	X	X	X	X	X	X	X	X	X	–
$^{186}W(n,\gamma)^{187}W$	–	X	–	–	–	–	–	–	–	–
$^{55}Mn(n,\gamma)^{56}W$	–	–	–	–	X	–	X	X	–	–

Conclusions

This paper is addressed to a general reader, who would be interested in the experiments contained in SINBAD–'fusion neutronics section'. It is also intended as a ready guide on the usefulness of the benchmark experiments for nuclear data validation. The synthesis of the quality assessment reports, released in the 2010 compilation of the database is presented. Interested readers are encouraged to search for further, more detailed and extensive information directly in the SINBAD database.

A shorthand note is finally released on any OKTAVIAN, FNS, FNG and TUD experiments, as it is in the quality assessment section of the 2010 SINBAD compilation. The claims follow the previous discussion, in the belief that they do not appear as 'self–assertive'.

The OKTAVIAN TUNGSTEN experiment seems to be of sufficient quality for nuclear data validation purposes. However, in order to use this benchmark for the validation of modern cross-section evaluations, supplementary experimental information would be needed on:

- the neutron realistic effects in the lower energy part of the spectrum (in particular the background subtraction method should be detailed),
- the gamma source measurements,
- the gamma detector response function.

The FNS TUNGSTEN experiment is ranked as benchmark quality experiment. However, supplementary experimental information would be needed on the effect of the experimental unfolding technique of the NE213 measurements and on the activation foils positioning, the corresponding uncertainty and housing

The FNG TUNGSTEN (integral) experiment is ranked as a benchmark quality experiment.

The FNG/TUD TUNGSTEN experiment could be ranked as a benchmark quality experiment, provided that supplementary experimental information is available on:

- the realistic and complete estimation of neutron and gamma flux point–wise uncertainties,
- availability of the original pulse-height distributions measured by spectrometers would be useful for those who wish to carry out their own spectra unfolding,
- some inconsistencies observed with the FNG–W (integral) benchmark results should be explained and resolved.

The OKTAVIAN SILICON 60 CM experiment can be ranked as a benchmark quality experiment for nuclear data validation purposes. In order to make a complete use of this benchmark experiment, supplementary experimental information is advisable on:

- the neutron realistic effects in the lower energy part of the spectrum (in particular the background subtraction method should be detailed),
- the gamma source measurements,
- the gamma detector response function.

The OKTAVIAN SILICON 40 CM experiment is ranked as a benchmark experiment of INTERMEDIATE quality because the neutron leakage flux measurements are only available in graphical form and their reading off is approximate.

The FNS GRAPHITE experiment is ranked as benchmark quality experiment. However, in order to use this benchmark for the validation of modern cross-section evaluations, supplementary experimental information would be needed on the effect of the experimental unfolding technique, activation foils positioning and housing

The FNG SILICON CARBIDE experiment is ranked as a benchmark quality experiment.

The FNG/TUD SILICON CARBIDE experiment could be ranked as a benchmark quality experiment, provided that supplementary experimental information is available on:

- realistic and complete estimation of neutron and gamma flux point–wise uncertainties,

- availability of the original pulse-height distributions measured by spectrometers would be useful for those who wish to carry out their own spectra unfolding,
- some inconsistencies observed with the FNG-SiC benchmark results should be explained and resolved.

The FNS VANADIUM experiment is ranked as a benchmark quality experiment. However, in order to use this benchmark for the validation of modern cross-section evaluations, supplementary experimental information would be needed on the effect of the experimental unfolding technique of the NE213 measurements and on the activation foils positioning, corresponding uncertainty and housing

The OKTAVIAN ALUMINIUM experiment is ranked as a benchmark quality experiment. However, in order to use this benchmark for the validation of modern cross-section evaluations, supplementary experimental information is advisable on:

- the neutron flight path parameter,
- the neutron realistic effects in the lower energy part of the spectrum (in particular the background subtraction method should be detailed),
- the gamma source measurements,
- the gamma detector response function.

The OKTAVIAN IRON experiment seems to be of sufficient quality for nuclear data validation purposes. However, the measurements should be used with caution because the uncertainties are very large.

The FNS IRON DOGLEG–DUCT experiment is ranked as an INTERMEDIATE quality benchmark experiment. Supplementary experimental information is needed on the neutron source spectrum. Likewise, supplementary experimental information would be useful on the neutron detector response function.

The TUD IRON SLAB experiment is ranked as benchmark quality experiment. It would be advisable to obtain more information on the source term.

The OKTAVIAN NICKEL experiment is of benchmark quality for nuclear data validation purposes.

The STAINLESS STEEL BULK SHIELD experiment is ranked as a benchmark quality experiment. However, the fact that the geometrical data are only given in the MCNP input format may pose problems for users of other codes. A comprehensive geometry description would be helpful.

The FNS OXYGEN experiment is ranked as a benchmark quality experiment. However, in order to use this benchmark for the validation of modern cross-section evaluations, supplementary experimental information would be needed on the neutron effective flight path parameter.

The TUD/FNG ITER Bulk Shield experiment could be ranked as benchmark quality experiment, provided that supplementary experimental information is made available on the realistic and complete estimation of neutron and gamma flux point–wise uncertainties; moreover, the original pulse-height distributions measured by spectrometers would be useful for those who wish to carry out their own spectra unfolding.

The ITER NEUTRON STREAMING experiment is ranked as a benchmark quality experiment.

The ITER DOSE RATE experiment is ranked as a benchmark quality experiment.

The FNS SKY–SHINE experiment could be ranked as a benchmark quality experiment, provided that supplementary information on the neutron source spectrum is supplied.

Acknowledgements

The paper is the synthesis of the outcomes from the quality assessment of the SINBAD experiments in 'Fusion Neutronics Section', supported by the Ministry of Science of Slovenia and by the OECD/NEA Data Bank. The authors wish to thank Dr. Enrico Sartori for the collaboration.

References

[1] Kodeli, I., E. Sartori, B. Kirk, "SINBAD Shielding Benchmark Experiments - Status and Planned", *Proc. of the American Nuclear Society's 14th Biennial Topical Meeting of the Radiation Protection and Shielding Division*, Carlsbad, New Mexico, USA, American Nuclear Society, ANS Order No. 700319 on CD, pp 87-92 (2006).

[2] Ichihara, C., *et al.*, "Measurement and Analysis of Neutron Leakage Spectra from Spherical assemblies of Chromium, Manganese and Copper with 14 MeV Neutrons", *Journal of Nuclear Science and Technology*, Vol. 37, No.4, p. 358-367 (2000).

[3] Yamamoto, J., *et al.*, "Gamma-Ray Emission Spectra from Spheres with 14 MeV Neutron Source", *Proceedings of the 1988 Seminar on Nuclear Data*, JAERI Report, JAERI-M 89-026, p. 232 (1989).

[4] Milocco, A., A. Trkov, I. Kodeli, "The OKTAVIAN TOF Experiments in SINBAD: Evaluation of the Experimental Uncertainties", *Annals of Nuclear Energy* 37, pp. 443-449 (2010).

[5] X–5 Monte Carlo Team, *MCNP–A General Monte Carlo N–Particle Transport Code, Version* 5, Volume I, II, III, April 24 (2003).

[6] Seki, Y., *et al.*, "Monte Carlo Calculations of Source Characteristics of FNS Water Cooled Type Tritium Target", *J. Nucl. Sci. Technol.*, 20, 686 (1983).

[7] Maekawa, F., *et al.*, *Compilation of Benchmark Results for Fusion Related Nuclear Data*, JAERI Report, JAERI-Data/Code 98-024 (1998).

[8] Trkov, A., *et al.*, "Progress in Evaluated Nuclear Data for Tungsten with Covariances", *Proc. of the International Conference on the Physics of Reactors "Nuclear Power: A Sustainable Resource"*, Interlaken, Switzerland (2008).